

Response to editor:

Dear Dr. Yugo Kanaya,

We thank you for the constructive comments and suggestions. We have revised the manuscript following the comments as described below. The comments are shown in blue. Our responses are shown in black. The revised texts are shown in italics.

1. The reviewer #1 requested discussion on how the uncertainty in emission inventories propagates into derived contributions. Although the uncertainties are added to Table in supplementary, no discussion is made. Key issues would be how NO_x and anthropogenic VOC concentrations are reproduced by the model simulations. I assume anthropogenic VOC concentrations are measurable from samples for isoprene and monoterpenes. If not, alternative way of evaluation should be proposed.

Thank you for pointing this out. We obtained anthropogenic emissions from the Multi-resolution Emission Inventory for China (Li et al., 2017), which is the most updated bottom-up emission inventory in China. We summarized the uncertainties of the bottom-up emissions in Table S1 in the latest revised manuscript.

As an important model input, emission estimates may largely impact simulated results. For NO_x, we evaluated the model performance by comparing with the observed hourly NO_x concentration at urban Xi'an (Table 3 and Figure 3). We found that our model successfully captured the observations of NO_x (with a mean bias of -0.4 ppb and NMB=-1%), which suggests no systematic bias in NO_x emissions. Unfortunately, the anthropogenic VOC was not included in our samples as the observations are primarily targeted to biogenic VOC in the Qinling forest. Alternatively, two sensitivity simulations are conducted in this revision (for 15th-17th August), namely RUN1 (with an increase of anthropogenic VOC emission by 50%) and RUN2 (with a decrease of anthropogenic VOC emission by 33%), to explore the sensitivity of simulated VOC and O₃ concentrations to anthropogenic VOC emissions. We found that 50% increases of anthropogenic VOC emission could lead to a 22% increase of urban VOC concentration, while the 33% emission decrease resulted in a 24% decrease of concentration (as shown in the table below). It is worth noting that the concentration of O₃ stayed almost the same (because the O₃ production regime is NO_x-limit). We addressed that the uncertainties of VOC emission obviously affected the VOC concentrations; however, MEIC inventory is the most updated available emission for China so far, and quantifying its uncertainties can be done in future studies (possibly with satellite-based measurement of HCHO (Miller et al., 2008)).

Species [ppb]	Base	RUN1	RUN2
O₃	40.7	41.9	39.8
Ethane	13.1	18.7	9.5
C>2 alkanes	11.2	16.1	8.9
HCHO	7.4	5.5	5.0
Acetaldehyde	5.4	4.7	4.2
Toluene	2.9	4.3	2.2

Ethene	2.8	4.2	2.3
Organic nitrogen	2.7	1.7	1.5
Organic peroxides	2.1	2.0	1.9
C>2 alkenes	2.0	3.2	1.7
Ketones	1.6	1.6	1.2
Xylenes	1.2	1.9	0.8
Organic acids	1.0	1.2	1.1
Total VOC	53.3	64.9	40.3

We added text in Section 2.3 and 3.3 to discuss about the uncertainties of emission estimates.

Section 2.3

5 *The emission estimates and uncertainties of VOCs, SO₂, NO_x, NH₃, and PM_{2.5} in the domain during the simulation period are summarized in Table S1, and the potential impacts of emission uncertainty on simulation will be discussed in Section 3.3.*

Section 3.3

10 *For NO_x, the simulated hourly NO_x averaged for the no-raining period was 46.6 ppb, close to the observed 47.0 ppb (NMB=-1%), which suggests no systematic bias in NO_x emissions....*

15 *Unfortunately, the anthropogenic VOC was not included in our samples as the observations are primarily targeted to biogenic VOC in the Qinling forest. Alternatively, two sensitivity simulations are conducted in this revision (for 15th-17th August), namely RUN1 (with an increase of anthropogenic VOC emission by 50%) and RUN2 (with a decrease of anthropogenic VOC emission by 33%), to explore the sensitivity of simulated VOC and O₃ concentrations to anthropogenic VOC emissions. We found that 50% increases of anthropogenic VOC emission could lead to a 22% increase of urban VOC concentration, while the 33% emission decrease resulted in a 24% decrease of concentration (Table S2). It is worth noting that the concentration of O₃ stayed almost the same (because the O₃ production regime is NO_x-limit). We addressed that the uncertainties of VOC emission obviously affected the VOC concentrations; however, MEIC inventory is the most updated available emission for*
20 *China so far, and quantifying its uncertainties can be done in future studies (possibly with satellite-based measurement of HCHO (Miller et al., 2008)).*
25

30 *2. Similarly, discussion on the potential impact from the isoprene chemical mechanism is still weak. The reviewer #1 requested justification why the new isoprene chemistry mechanism does not impact the results. However such justification is not present, although impact in other studies is cited. The authors mentioned "the impacts of biogenic VOCs on O₃ formation may vary in different regions and different seasons." The impact of new isoprene chemistry mechanism could be different too, and therefore case study for Guanzhong Basin is necessary.*

35 *Thanks for the comment. We updated the RADM2 mechanism to include the*

new isoprene chemistry as follows:



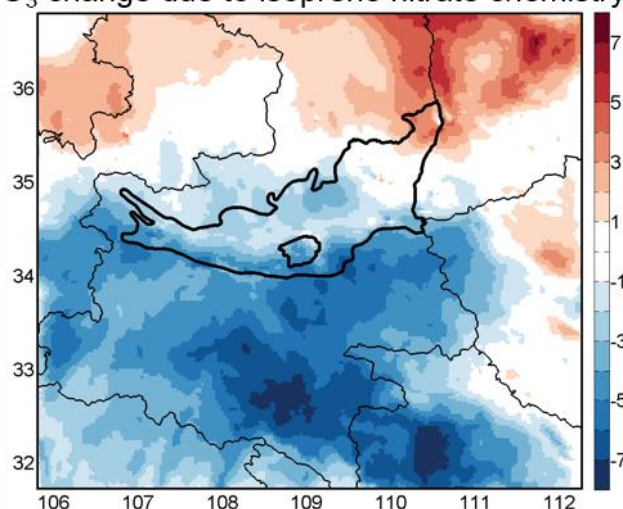
5 where, ISOPO₂ represents the hydroperoxy radical from isoprene, ISOPN represents the organic nitrate.

Many laboratory, filed observations and simulation studies (e.g. von Kuhlmann et al., 2004; Perring et al., 2009; Paulot et al., 2009a; Fisher et al., 2016; Travis et al., 2016) all agreed that tropospheric O₃ production was highly sensitive to the ISOPN yield (4% to 15%) and large uncertainties still remained. Horowitz et al. (2007) found a 4% ISOPN yield best captured the alkyl and multifunctional nitrates measured by aircraft, and Hudman et al. (2009) pointed out that unreasonably high ISOPN yield (18%) would let ISOPN be a terminal sink for NO_x. Here, we adopted the ISOPN yield to be 4% followed Horowitz et al. (2007) and the rate constant to be $2.7 \times 10^{-12} \times \exp(350/T)$ followed MCM3.1. We conducted a 3-day simulation (15th -17th Aug.) to evaluate the potential impacts of this new isoprene chemistry. The simulated results show that near surface O₃ concentration decrease by 2-8 ppb over the Qinling Mountains (the region with high isoprene concentration) and increase by 1-5 ppb in the northeast of the Guanzhong basin (impact of the transport of ISOPN). In the urban Xi'an, the averaged O₃ concentration decreased by 3 ppb (8%). It could be interesting for our future work to conduct a more detailed analysis about the sensitivity and uncertainties of the ISOPN yield, as well as NO_x recycling.

We added the discussion above in Section 2.2 to state the potential uncertainty.

We noted some advances in isoprene nitrate chemistry in recent years. Some studies pointed out that isoprene reacts with OH radical to form hydroperoxy radicals (ISOPO₂). Subsequently, in the presence of NO_x, ISOPO₂ reacts with NO leading to the production of hydroxynitrates (ISOPN) by a minor branch, which sequesters NO_x and therefore regulates O₃ formation. A number of laboratory, filed observation and simulation studies (e.g. Paulot et al., 2009a, b, 2012; Horowitz et al., 2007; Hudman et al., 2009; Fisher et al., 2016; Travis et al., 2016) highlighted the importance of isoprene nitrate chemistry and all agreed there were still large uncertainties (for example, the estimates of ISOPN yield (4%-15%)). Horowitz et al. (2007) found a 4% ISOPN yield best captured the alkyl and multifunctional nitrates measured by aircraft, and Hudman et al. (2009) pointed out that unreasonably high ISOPN yield (18%) would let ISOPN be a terminal sink for NO_x. Back to our study, this isoprene nitrate chemistry was not contained in the standard RADM2 mechanism. To assess the potential uncertainties, we modified the RADM2 mechanism by adding formation pathway of ISOPN from ISOPO₂+NO, and run a 3-day (15th -17th August) simulation to quantify the impacts in the GZ basin. We adopted the ISOPN yield to be 4% followed Horowitz et al. (2007) and the rate constant to be $2.7 \times 10^{-12} \times \exp(350/T)$ followed MCM3.1. A 8% (3 ppb) decrease of the near surface O₃ concentration was found averaged for urban Xi'an in August after implementing the updated isoprene nitrate chemistry.

O₃ change due to isoprene nitrate chemistry



3. The authors mentioned that sampling was conducted between 9:30-16:30 LT. Were the sampling CONTINUED for 7 hours? Or the short-time samplings were done during the period? Clarification is necessary.

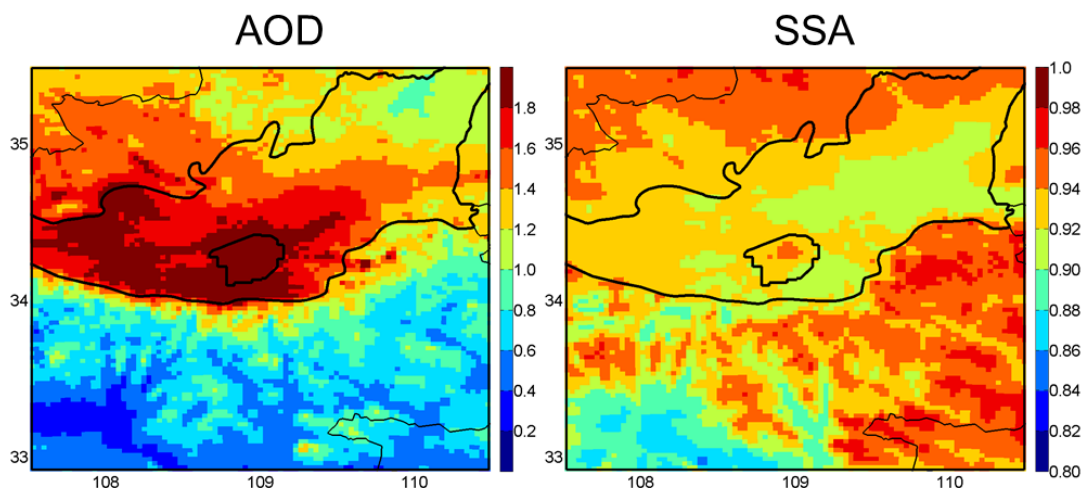
We appreciate the editor's concern. Each sampling duration was 30 minutes during 9:30 am to 16:30 pm local time. We modified the text in Section 2.1.1 to make our statement more clear.

10 *Sampling was conducted between 9:30 am to 16:30 pm local time (each sampling lasted for 30 minutes) to target expected daily maximum isoprene concentrations.*

15 4. Point 3 of reviewer #2. I also feel impact of aerosols (that the authors claim) on $J(\text{NO}_2)$, 40-60%, is a bit too large. TUV calculations (http://cprm.acom.ucar.edu/Models/TUV/Interactive_TUV/) to yield 40% lower $J(\text{NO}_2)$ require AOD=1 and single scattering albedo (SSA) =0.8, or AOD=2 and SSA=0.93. The authors should raise AOD (in addition to PM) and expected SSA during the studied period, to justify that large impact.

20 Thanks for the suggestion. We calculated the AOD and SSA at 550 nm in the GZ basin during 15th-30rd August, excluding rainy days. The figure below shows the spatial distribution of the simulated results. The AOD averaged for urban Xi'an is 1.92, and SSA is 0.92. We modified the text in Section 4.1 to describe this issue.

25 *In the daytime, NO_2 photolysis frequency ($J(\text{NO}_2)$) is determined by the solar radiation influenced by PM via scattering and absorption. Figure 6 shows the changes of $J(\text{NO}_2)$ (calculated by model track output *photor_no2*) with the participation of PM (concentration, $102 \mu\text{g m}^{-3}$; aerosol optical depth (AOD) at 550 nm, 1.92; single scattering albedo (SSA) at 550 nm, 0.92) averaged for urban Xi'an. $J(\text{NO}_2)$ was reduced by 40-60%, most significantly in morning and evening rush hours.*



5. Section 4.1. Is the unit for VOCs ppb or ppbC? What are the dominant VOCs for 50 or 30 ppb that the authors discussed?

5 We appreciate the editor's concern. The unit for VOC is ppb. The dominant VOC in urban Xi'an (the 50 ppb) is ethane, and the domain VOC among the Qinling Mountains (the 30 ppb) is isoprene. We modified the text in Section 4.1 to discuss the issue.

10 *Figure 4a shows spatial distribution of the simulated VOCs during the no-raining period, overlaid with the simulated wind vectors. The highest concentration (more than 50 ppb, with ethane being the dominant species) was in urban Xi'an and its downwind region (the southwest of urban Xi'an), due to anthropogenic activities. In addition, another high-value area (~30 ppb, with isoprene being the dominant species) was found in the Qinling Mountains, which was probably*
 15 *due to biogenic sources.*

Reference

- 20 Fisher, J.A., Jacob, D.J., Travis, K.R., Kim, P.S., Marais, E.A., Miller, C.C., Yu, K., Zhu, L., Yantosca, R.M., and Sulprizio, M.P.: Organic nitrate chemistry and its implications for nitrogen budgets in an isoprene- and monoterpene-rich atmosphere: constraints from aircraft (SEAC4RS) and ground-based (SOAS) observations in the Southeast US, *Atmos. Chem. Phys.*, 16, 1-38, doi: 10.5194/acp-16-5969-2016, 2016.
- 25 Horowitz, L. W., Fiore, A.M., Milly, G.P., Cohen, R.C., Perring, A., Wooldridge, P.J., Hess, P.G., Emmons, L.K., and Lamarque J.F.: Observational constraints on the chemistry of isoprene nitrates over the eastern United States, *J. Geophys. Res.*, 112, D12S08, doi:10.1029/2006JD007747, 2007.
- 30 Hudman, R.C., Murray, L.T., Jacob, D.J., Turquety, S., Wu, S., Millet, D.B., Avery, M., Goldstein, A.H., and Holloway, J.: North American influence on tropospheric ozone and the effects of recent emission reductions: Constraints from ICARTT observations, *J. Geophys. Res.*, 114, D07302, doi:10.1029/2008JD010126, 2009.

- Li, M., Zhang, Q., Kurokawa, J.I., Woo, J.H., He, K., Lu, Z., Ohara, T., Song, Y., Streets, D.G., Carmichael, G.R., Cheng, Y., Hong, C., Huo, H., Jiang, X., Kang, S., Liu, F., Su, H., and Zheng, B.: MIX: a mosaic Asian anthropogenic emission inventory under the international collaboration framework of the MICS-Asia and HTAP, *Atmos. Chem. Phys.*, 17, 935-963, doi:10.5194/acp-17-935-2017, 2017.
- 5 Millet, D.B., Jacob, D.J., Boersma, K.F., Fu, T.M., Kurosu, T.P., Chance, K., Heald, C.L., and Guenther, A.: Spatial distribution of isoprene emissions from North America derived from formaldehyde column measurements by the OMI satellite sensor, *J. Geophys. Res.*, 113, D02307, doi:10.1029/2007JD008950, 2008.
- 10 Paulot, F., Crouse, J.D., Kjaergaard, H.G., Kroll, J.H., Seinfeld, J.H., and Wennberg, P.O.: Isoprene photooxidation: New insights into the production of acids and organic nitrates, *Atmos. Chem. Phys.*, 9(4), 1479–1501, 2009a.
- Paulot, F., Crouse, J.D., Kjaergaard, H.G., Kurten, A., St Clair, J.M., Seinfeld, J.H., and Wennberg, P.O.: Unexpected epoxide formation in the gas-phase photooxidation of isoprene, *Science*, 325(5941), 730–733, 2009b.
- 15 Perring, A.E., Wisthaler, A., Graus, M., Wooldridge, P.J., Lockwood, A.L., Mielke, L.H., Shepson, P.B., Hansel, A., and Cohen, R.C.: A product study of the isoprene + NO₃ reaction, *Atmos. Chem. Phys.*, 9(14), 4945–4956, 2009.
- Travis, K.R., Jacob, D.J., Fisher, J.A., Kim, P.S., Marais, E.A., Zhu, L., Yu, K., Miller, C.C., Yantosca, R.M., Sulprizio, M.P., Thompson, A.M., Wennberg, P.O., Crouse, J.D., St Clair, J.M., Cohen, R.C., Laughner, J.L., Dibb, J.E., Hall, S.R., Ullmann, K., Wolfe, G.M., Pollack, I.B., Peischl, J., Neuman, J.A., and Zhou, X.: Why do models overestimate surface ozone in the Southeast United States? *Atmos. Chem. Phys.*, 16, 13561-13577, doi:10.5194/acp-16-13561-2016, 2016.
- 20 von Kuhlmann, R., Lawrence, M.G., Poschl, U., and Crutzen, P.J.: Sensitivities in global scale modeling of isoprene, *Atmos. Chem. Phys.*, 4, 1–17, 2004.
- 25

**Impacts of Biogenic and Anthropogenic Emissions on Summertime
Ozone Formation in the Guanzhong Basin, China**

Nan Li ^{1,2}, Qingyang He ^{2,3}, Jim Greenberg ⁴, Alex Guenther ⁵, Junji Cao ^{2,6}, Jun Wang ⁷, Hong Liao ¹, **Qiyuan Wang** ², Qiang Zhang ⁸

¹Jiangsu Key Laboratory of Atmospheric Environment Monitoring and Pollution Control, Jiangsu Collaborative Innovation Center of Atmospheric Environment and Equipment Technology, School of Environmental Science and Engineering, Nanjing University of Information Science & Technology, Nanjing, 210044, China

²Key Lab of Aerosol Chemistry & Physics, SKLLQG, Institute of Earth Environment, Chinese Academy of Sciences, Xi'an, 710061, China

³Nanjing Star-jelly Environmental Consultants Co., Ltd, Nanjing, 210013, China

⁴National Center for Atmospheric Research, CO, USA

⁵Department of Earth System Science, University of California, Irvine, Irvine CA 92697-3100, USA

⁶Institute of Global Environmental Change, Xi'an Jiaotong University, Xi'an, 710049, China

⁷Center of Global and Regional Environmental Research, Department of Chemical and Biochemical Engineering, University of Iowa, Iowa City, Iowa, USA

⁸Department of Earth System Science, Tsinghua University, Beijing, 100084, China

25

Correspondence to: Nan Li, linan@nuist.edu.cn

Abstract

This study is the first attempt to understand the synergistic impact of anthropogenic and biogenic emissions on summertime ozone (O₃) formation in the Guanzhong (GZ) basin where Xi'an, the oldest and the most populous city (with a population of 9 million) in the northwest China, is located. Month-long (August 2011) WRF-Chem simulations with different sensitivity experiments were conducted and compared with near-surface measurements. Biogenic volatile organic compounds (VOCs) concentrations were characterized from 6 surface sites among the Qinling Mountains, and urban air composition was measured in the Xi'an city at a tower 100 m above the surface. The WRF-Chem control experiment reasonably reproduced the magnitudes and variations of observed O₃, VOCs, NO_x, PM_{2.5} and meteorological parameters, with normalized mean biases for each parameter within $\pm 21\%$. Subsequent analysis employed the factor separation approach (FSA) to quantitatively disentangle the pure and synergistic impacts of anthropogenic and/or biogenic sources on summertime O₃ formation. The impact of anthropogenic sources alone was found to be dominant for O₃ formation. Although anthropogenic particles reduced NO₂ photolysis by up to 60%, the anthropogenic sources contributed 19.1 ppb O₃ formation on average for urban Xi'an. The abundant biogenic VOCs from the nearby forests promoted O₃ formation in urban areas by interacting with the anthropogenic NO_x. The calculated synergistic contribution (from both biogenic and anthropogenic sources) was up to 14.4 ppb in urban Xi'an, peaking in the afternoon. Our study reveals that the synergistic impact of individual source contributions to O₃ formation should be considered in the formation of air pollution control strategies, especially for big cities in the vicinity of forests.

25

Keywords: ozone, emission, biogenic volatile organic compounds, WRF-Chem

1. Introduction

Elevated ozone (O_3) levels in China has drawn increasing attention in recent years (e.g. Xue et al., 2014; Hu et al., 2016; Wang T. et al., 2016; Wang M. et al., 2016). O_3 , a secondary pollutant, is mainly formed by complex photochemical reactions of nitrogen oxides ($NO_x = NO + NO_2$) and volatile organic compounds (VOCs). High O_3 concentration at ground level is harmful to human health and ecosystems (WHO, 2005; Feng et al., 2015; Brauer et al., 2016). O_3 in the troposphere is an important greenhouse gas that has the third-highest radiative forcing after CO_2 and CH_4 (Stevenson et al., 2013; IPCC, 2013). In addition, O_3 is the primary source of the hydroxyl radical (OH), which has a major influence on the oxidizing capacity of the atmosphere and thus impacts the oxidation chemistry of secondary pollutants (e.g. sulfate and secondary organic aerosol) (Ehhalt et al., 2000; Rohrer et al., 2006). In recent years, the surface O_3 level has been increasing in most Chinese cities. For instance, in the highly urbanized areas in China, maximum 8h O_3 concentration increased by 19% (16.9 ppb) from 2015 to 2017 in the Beijing-Tianji-Hebei (BTH) region, the growth trend was 14% (11.3 ppb) for the Pearl River Delta (PRD) region and 12% (10.5 ppb) for the Yangtze River Delta (YRD) region (<http://datacenter.mep.gov.cn>). In the future, the pollution trend is likely to worsen due to potential changes of climate and emissions (Wang et al., 2013; Liu et al., 2013; Zhu et al., 2016, 2017).

On the global scale, VOC emissions from natural vegetation is estimated to be one order greater than that from anthropogenic activities, in spite of large uncertainties in different studies (Guenther et al., 2006; Wu et al., 2007, 2008; Jiang et al., 2013; Zhu et al., 2017). In addition, biogenic VOCs (e.g. isoprene) are highly reactive, reacting more efficiently with OH than most anthropogenic VOC species (Carlo et al., 2004). Previous studies have demonstrated the significant impacts of biogenic VOCs on surface O_3 formation under strong solar radiation, high temperature and NO_x level (e.g. Fiore et al., 2005, 2011; Wang et al., 2008; Curci et al., 2009; Geng et al., 2011; Strong et al., 2013; Squire et al., 2014; Lee et al., 2014; Zhang et al., 2017). In China, biogenic VOC emissions are estimated to be 17-44 TgC yr^{-1} (Guenther et al., 1995; Lin et al., 2008; Fu et al., 2012, 2104; Li et al., 2014), and are concentrated in the warm summer season. Current studies report that biogenic VOCs contribute to surface O_3 concentrations in China (Geng et al., 2011; Qu et al.,

2013, 2014) and play an important role in intercontinental transport of O₃ (Zhu et al., 2017).

The impacts of biogenic VOCs on O₃ formation may vary in different regions and different seasons (Im et al., 2011; Strong et al., 2013; Wagner et al., 2014; Lee et al., 2014). Qu et al. (2013) employed the RAQM model to examine the influence of biogenic emissions on daily maximum surface O₃ concentration in China. Their calculations showed that in general the impact from biogenic sources on O₃ were more obvious in South China than in North China, but the O₃ increments in different regions didn't follow the same seasonality. Geng et al. (2011) used the WRF-Chem model to evaluate the effect of biogenic emissions on O₃ production in Shanghai in summer, and suggested that the carbonyls produced by the continuous oxidation of isoprene have important impacts on O₃ level in the city. In addition, some studies suggest that biogenic emissions may increase due to global warming and land-use change, and the impact on O₃ formation could be more significant in the future (Lin et al., 2008; Fiore et al., 2011; Liu et al., 2013; Fu et al., 2015). Fiore et al. (2011) pointed out that the potential increases in biogenic isoprene in North American (NA) could offset the regional and intercontinental surface O₃ decreases produced by controls on NA anthropogenic emissions during warm seasons.

The Guanzhong (GZ) basin is the most developed region in northwestern China. In the past few years, air pollution has grown up to be a severe issue in the GZ basin (Wang et al., 2012; Xue et al., 2017), due to its specific basin topography and abundant anthropogenic emissions (Li et al., 2017). According to the data from national environmental monitoring stations in the GZ basin, 43% of days in 2013-2017 have AQI > 100 (e.g., unhealthy air quality category), and in summer O₃ was regarded as the primary pollutant in 70% of polluted cases. In this study, we employed a regional chemical model WRF-Chem to simulate O₃ concentration in the GZ basin for summer 2011. Our aim is the source apportionment of urban O₃ formation in this city surrounded by forests, specifically quantifying the individual and synergistic contributions of anthropogenic and biogenic sources. The paper is organized as follows. We first describe the sampling campaign, the chemical model and the emission data used for driving the model (Section 2). We then evaluate the model performance by comparing the observed urban air quality and biogenic VOCs with the simulated results (Section 3). Finally, we analyze the sensitivity of

summertime O₃ formation to biogenic and anthropogenic sources (Section 4).

2. Methodology

2.1 Sampling sites and descriptions

5 The study was conducted in Xi'an, one of the oldest cities in the world. Xi'an is
the most populous city in the northwest of China with a population of greater than 9
million. It is located in the heartland of the GZ basin between the Qinling Mountains
and the Loess Plateau (Fig. 1). The topographical features result in air pollutants often
being trapped in the valley with limited dispersion. The city borders the northern foot
10 of the Qinling Mountains, only around 50 kilometers from downtown to the foothills.
The Qinling Mountains are an east-west mountain range of 1600 kilometers in length
and 300 kilometers in width and are regarded as a natural boundary between Northern
and Southern China. Climate, and even culture are significantly different from the
north to the south. The Xi'an city has high temperatures and strong solar intensity in
15 summer, making it an ideal location to assess the importance of biogenic contributions
to urban air quality.

2.1.1 Biogenic VOC measurements in the Qinling Mountains

We selected six field sites in the Qinling Mountains (Fig. 1b, the triangles) and
collected one ambient air sample at each site on 6th – 7th August 2011 under sunny
20 weather conditions (details are presented in Table 1). Sampling was conducted
between 9:30 am to 16:30 pm local time (each sampling lasted for 30 minutes) to
target expected daily maximum isoprene concentrations. At each site, ambient air
samples were pulled in parallel onto three cartridges filled with Tenax GR and
Carbograph 5TD solid adsorbents using a mass flow controlled pump for 30 min.
25 Samples were shipped to the lab at NCAR (Boulder CO, USA) for chemical analysis.
Cartridges were desorbed using an UltraTM TD auto sampler with a Unity thermal
desorption system (MARKES International Series 2, Llantrisant, UK) interfaced with
a temperature programmed Agilent 7890A series Gas Chromatograph with a 5975C
Electron Impact Mass Spectrometer and a Flame Ionization Detector (GC-MS/FID,
30 Agilent Technologies, Santa Clara, CA, USA). We used nitrogen as a carrier gas at the
flow rate of 3 mL min⁻¹. Isoprene and monoterpene identifications were based on the

comparison of retention time of authentic standards and mass spectra in the National Institute of Standards and Technologies (NIST) databases. Quantifications were calculated using FID calibrated with a NIST traceable standard.

2.1.2 Air quality monitoring in urban Xi'an

5 We set up an urban air quality monitoring site (Fig. 1b) at the roof (107 m above ground) of the main building (108.984°E, 34.245°N) on the campus of Xi'an Jiaotong University to minimize the ground level influences of local emissions. The campus is in the southeastern part of the downtown surrounded by residential areas. We obtained reliable observations of the concentrations of O₃, NO_x and PM_{2.5} during 15th – 30th
10 August 2011. Gases were measured by Ecotech analyzers (Ecotech Pty Ltd, Australia). O₃ were measured by an UV photometric analyzer EC9801. NO_x was measured by a gas-phase chemiluminescence detection analyzer EC9841, coupled with a hot molybdenum converter. We collected 24h PM_{2.5} filter samples by a mini-volume sampler (Airmetrics, USA) at a flow rate of 5 L min⁻¹ using both 47 mm quartz-fiber
15 (Whatman, Mid-dlesex, UK) and teflon-membrane (Gelman, Ann Arbor, MI) filters. We calculated the PM_{2.5} mass concentrations gravimetrically by weighing the teflon-membrane filters pre and post-collection for at least 4 times using an electronic microbalance (MC5, Sartorius, Göttingen, Germany) with ±1 µg sensitivity under controlled conditions. EC and OC concentrations were analyzed based on a 0.5 cm²
20 punch from the quartz-fiber filter following the IMPROVE_A (Interagency Monitoring of Protected Visual Environments) thermal/optical reflectance (TOR) protocol (Chow et al., 2007) using a DRI model 2001 Carbon Analyzer. The concentrations of ions were quantified from a 10.8 cm² of the teflon-membrane filter
25 by a Dionex DX-600 ion chromatography (Dionex Inc., Sunnyvale, CA, USA) (Zhang et al., 2014).

2.2 The WRF-Chem model

We employed the WRF-Chem model to study biogenic VOC emissions from the Qinling Mountains and their contributions to regional O₃ formation in urban Xi'an.
30 WRF-Chem is a 3-D online-coupled meteorology and chemistry model consisting of the components of emission, transport, chemical transformation, photolysis and radiation (Tie et al., 2003, Li et al., 2011), dry and wet deposition (Wesely, 1989), and

aerosol interactions (replaced with CMAQ aerosol module, Binkowski and Roselle, 2003; Li et al., 2010). WRF is a non-hydrostatic mesoscale dynamical system with various options for physical parameterizations (Skamarock et al., 2008). The chemical modules were implemented into the WRF framework obeying the same schemes for the simultaneous simulations (Grell et al., 2005).

We adopted RADM2 (Regional Acid Deposition Model) as the gas phase chemical mechanism to predict O₃ formation. RADM2 is an aggregated species type using the reactivity based weighting scheme to adjust for lumping (Stockwell et al., 1990). The mechanism implemented in our WRF-Chem model covers 158 reactions among 36 species, containing the complete reaction paths for isoprene, monoterpenes and the relevant inorganic reactions. As an explicit species, isoprene chemistry is based on an updated CB4 gas-phase mechanism (Carter and Atkinson., 1996). We noted some advances in isoprene nitrate chemistry in recent years. Some studies pointed out that isoprene reacts with OH radical to form hydroperoxy radicals (ISOPO₂). Subsequently, in the presence of NO_x, ISOPO₂ reacts with NO leading to the production of hydroxynitrates (ISOPN) by a minor branch, which sequesters NO_x and therefore regulates O₃ formation. A number of laboratory, field observation and simulation studies (e.g. Paulot et al., 2009a, b, 2012; Horowitz et al., 2007; Hudman et al., 2009; Fisher et al., 2016; Travis et al., 2016) highlighted the importance of isoprene nitrate chemistry and all agreed there were still large uncertainties (for example, the estimates of ISOPN yield (4%-15%)). Horowitz et al. (2007) found a 4% ISOPN yield best captured the alkyl and multifunctional nitrates measured by aircraft, and Hudman et al. (2009) pointed out that unreasonably high ISOPN yield (18%) would let ISOPN be a terminal sink for NO_x. Back to our study, this isoprene nitrate chemistry was not contained in the standard RADM2 mechanism. To assess the potential uncertainties, we modified the RADM2 mechanism by adding formation pathway of ISOPN from ISOPO₂+NO, and run a 3-day (15th-17th August) simulation to quantify the impacts in the GZ basin. We adopted the ISOPN yield to be 4% followed Horowitz et al. (2007) and the rate constant to be $2.7 \times 10^{-12} \times \exp(350/T)$ followed MCM3.1. A 8% (3 ppb) decrease of the near surface O₃ concentration was found averaged for urban Xi'an in August after implementing the updated isoprene nitrate chemistry.

The simulated domain (Fig. 1) is 600×600 km² centered on urban Xi'an with 3 km

horizontal grid spacing. We set up 28 vertical layers from the surface up to 50 hPa with 7 layers below 1 km to assure a high near-ground vertical resolution. The National Centers for Environmental Prediction (NCEP) FNL Operational Global Analysis data provided the initial and boundary fields of meteorology. Initial and boundary conditions of chemistry were derived by a global chemical transport model (Model for Ozone and Related chemical Tracers, MOZART) (Emmons et al., 2010). We considered the first 7 days as spin-up period, and the study focused on 6th – 7th and 15th – 30th August 2011 because of the available field observation datasets (as described in Section 2.1).

10

2.3 Biogenic and anthropogenic emissions

Biogenic emissions were quantified by the widely used model MEGAN (Model of Emissions of Gas and Aerosols from Nature) (Guenther et al., 2006). MEGAN coupled into the WRF-Chem model, referred to here as WRF-MEGAN2, provides on-line estimates of the net landscape-averaged biogenic emissions from terrestrial ecosystems into the above-canopy atmosphere. The on-line estimated emissions of isoprene, individual monoterpenes and other biogenic VOCs serve as the inputs for the further chemistry simulation. To drive MEGAN, we need the following inputs: emission factors (EFs), leaf area index (LAI), plant functional types (PFTs), as well as meteorology conditions. The meteorology was obtained from WRF simulations and the LAI and PFT data were extracted from MODIS (Tian et al., 2004). We adopted the canopy-scale emission factors of dominant species from Guenther et al. (2006).

Estimated the whole year 2011 by WRF-MEGAN2, the isoprene and monoterpene emissions in the Qinling Mountains were mostly concentrated in summer (71% and 58%, respectively). During our simulation period, the isoprene emission from the domain is 157 Gg mon⁻¹, accounting for ~80% of total biogenic VOC emissions (Table S1). The rest are monoterpenes and other biogenic VOCs (e.g. acetone and MBO (2-methyl-3-buten-2-ol)). Figures 2a and 2b show the spatial distributions of biogenic isoprene and monoterpenes emission fluxes during the simulation period, indicating the high emission zone of isoprene in the Qinling Mountains lying to the south of the Xi'an city.

The anthropogenic emissions were obtained from the Multi-resolution Emission

Inventory for China (MEIC, [Li et al., 2017](#)) for the year of 2010, which was downscaled to a resolution of 3 km using locations of point sources and various spatial proxies (Geng et al., 2017). The upgraded highly resolved emission data were based on a collection of statistics and newly developed emission factors. The emission inventory used in our model includes all major anthropogenic sources, but excluded open biomass burning which occupies a low proportion in the GZ basin during our simulating period (estimated by Fire Inventory from NCAR, <https://www2.acom.ucar.edu/modeling/finn-fire-inventory-ncar>). The anthropogenic emission sources are composed of power, industry, residential, transportation, and agriculture. **The emission estimates and uncertainties of VOCs, SO₂, NO_x, NH₃, and PM_{2.5} in the domain during the simulation period are summarized in Table S1, and the potential impacts of emission uncertainty on simulation will be discussed in Section 3.3.** The estimated anthropogenic VOCs emissions are 72.2 Gg, contributing up to ~30% of total VOC emissions. Figures 2c and 2d present the spatial distributions of anthropogenic VOC and NO_x emissions in the simulation period. The highest emission intensity of anthropogenic VOCs and NO_x are in Xi'an city and the GZ basin due to the frequent vehicle and industrial activities of this area.

2.4 Factor Separation Technique

O₃ is formed by complicated nonlinear reactions of anthropogenic and biogenic precursors (NO_x and VOCs) in the presence of sunlight. **The approach referred to as the “brute-force” method (sensitivity analysis used to measure the model output response to emission changes) is traditionally used in air quality model to identify source contributions from specific non-reactive species in a linear process, but it cannot straightforward apply to secondary species due to the non-linearity in responses.** In practice, the actual impact of one factor in a nonlinear process in the presence of others can be separated into 1) pure impact from the factor and 2) interactional impacts from all those factors. In this study, we adopted the factor separation approach (FSA) (Stein and Alpert, 1993) to decompose the pure contribution of a factor from its interaction with other factors.

We considered anthropogenic and biogenic sources as two interactional factors to influence the O₃ formation. $f_{\text{anth-bio}}$, f_{anth} , f_{bio} and f_0 are the simulation results including

both anthropogenic and biogenic sources, anthropogenic source only, biogenic source only, and neither, respectively. Pure contributions of anthropogenic and biogenic sources are expressed as Eq. (1) and (2), respectively:

$$f'_{anth} = f_{anth} - f_0 \quad (1)$$

$$f'_{bio} = f_{bio} - f_0 \quad (2)$$

The calculated result including both anthropogenic and biogenic sources should include both pure contributions of the two factors, the synergistic impact, and the impact of background transport (Eq. 3):

$$f_{anth-bio} = f'_{anth} + f'_{bio} + f_{anth-bio} + f_0 \quad (3)$$

Thus, the synergistic effect between anthropogenic and biogenic sources is represented as:

$$\begin{aligned} f'_{anth-bio} &= f_{anth-bio} - f'_{anth} - f'_{bio} - f_0 \\ &= f_{anth-bio} - (f_{anth} - f_0) - (f_{bio} - f_0) - f_0 \\ &= f_{anth-bio} - f_{anth} - f_{bio} + f_0 \end{aligned} \quad (4)$$

Based on the FSA, we conducted four simulations, namely BASE, ANTH, BIO and NEITHER, to explore the pure and synergistic impacts of anthropogenic and/or biogenic sources on O₃ production in the GZ basin. Detailed simulation settings and the various contribution definitions are summarized in Table 2.

3. Observation data and model validation

3.1 Meteorology

The specific topographical features of Xi'an make the meteorological conditions crucial for the accumulation and dispersion of urban pollutants. To validate our model performance in wind, temperature and relative humidity, we compared the hourly meteorological data (<http://www.meteomanz.com>) observed at the Jinghe site (108.58°E, 34.26°N, in the west of Xi'an) with model simulations. Figure 3c illustrates the observed and simulated near-surface wind speed and directions during 15th – 30th August 2011. The WRF-Chem model successfully captured the prevailing wind direction from north and northeast, consistent with the in-situ observations. It should be noted that in our simulation period the prevailing wind blew from south, which enhanced the transport of biogenic emissions from the Qinling Mountains to

urban Xi'an. In addition, a continuous rainfall event during 18th-22nd August (green shadow in Fig. 3) was characterized by lower temperature and near-saturated humidity.

We conducted the statistical verification of meteorological variables in Table 3, including the r (correlation coefficient), NMB (normalized mean bias) and RMSE (root mean square errors). Modeled meteorological variables were in good agreement with observations (Fig. 3a-c) with the NMB less than $\pm 6\%$.

3.2 Biogenic VOC concentrations in the Qinling Mountains

Samples from the Qinling Mountains show that the dominant VOC species was isoprene, and α -pinene was the main constituent of monoterpenes (Table 1). The ratio of isoprene to monoterpenes varies considerably. In general, different terpene emitters are not homogeneously distributed in a kilometer-scale grid and the point measurements are influenced by the microenvironment and meteorology (Zare et al., 2012; Kota et al., 2015). However, in this study, our goal is to estimate the biogenic effects on urban O₃ 50 km away from the foothills, which requests more concern on the regional scale VOC level, rather than the microenvironment-scale variability in either the observation or the simulation. Thus, we compared the average of VOC measurements with model simulations to validate whether the calculated results were reasonable. The isoprene mean concentration simulated in the six grids (corresponding to the time of observations) was 1.4 ppb, which is close to the observed average value of 1.3 ppb at the six sampling sites. Monoterpenes performed quite similarly, simulated 0.22 ppb comparing with observed 0.21 ppb. We also analyzed the temporal variation of simulated biogenic VOC during the whole simulation period and found the sub-month variability was relatively small (the standard deviation < 25%). The evaluation indicates that biogenic VOCs simulations reasonably agreed with the observations in the Qinling Mountains, on average, which provides a basis for us to further evaluate biogenic effects on O₃.

3.3 Gaseous and particulate pollutants in urban Xi'an

The sampling campaign was organized in summer. Based on the gaseous and

particulate pollutant observations, the daily mean PM_{2.5} concentration was 90.0±53.5 μg m⁻³, with 57% of days exceeding the WHO Interim target-1 (IT-1) 75 μg m⁻³. The daily mean NO_x concentrations were 25.8-63.2 ppb, with 40% of days exceeding the guideline 48.7 ppb (≈100 μg m⁻³, GB 3095-2012). The maximum 8h O₃ concentration was 3.5-95.6 ppb, with most of the values around the national first grade standard of 46.6 ppb (≈100 μg m⁻³, GB 3095-2012). Summer in Xi'an is monitored as the least polluted season of the year, and the case we picked is regarded as a typical situation in summer Xi'an.

Figure 3 compares the simulated hourly O₃ and NO_x concentrations with in-situ observations. During the rainy episode (the green shadow in Fig. 3), our model overestimated NO_x concentration and underestimated O₃ concentration. The deviation can be explained by the failure to simulate the precipitation in the WRF model resulting in underestimates in wet deposition. So, we focused our analysis on the period excluding the rainy period. During the no-raining days, our model well reproduced the diurnal variations and magnitudes of O₃ and NO_x concentrations. The calculated O₃ averaged for no-raining period was 38.7 ppb, ~20% higher than the observed value of 31.5 ppb. Our simulated O₃ also reproduced the temporal variation of the observed O₃ (r = 0.72). For NO_x, the simulated hourly NO_x averaged for the no-raining period was 46.6 ppb, close to the observed 47.0 ppb (NMB=-1%), which suggests no systematic bias in NO_x emissions. It is worth noting that the observed NO_x were detected by a chemiluminescence analyzer coupled with a hot molybdenum converter (MoO), and this method was recognized to cause higher NO₂ concentration due to the positive interference of other nitrogen-containing components (NO_z, e.g. PAN, HNO₃ and HONO). Xu et al. (2013) found that the uncertainty caused by the MoO converter was much smaller at urban sites (less than 10%) than that at suburban and background sites (more than 30%). In the GZ basin, to evaluate the uncertainty, we estimated the ratio of NO_z/(NO_x+NO_z) from the model. The calculated results indicated that the NO_z accounted for 11% of the total NO_x+NO_z at urban Xi'an during the no-raining period. We noted the uncertainty in our NO_x measurements, but considered this would not crucially impact the model-measurement comparison.

Unfortunately, the anthropogenic VOC was not included in our samples as the observations are primarily targeted to biogenic VOC in the Qinling forest. Alternatively, two sensitivity simulations are conducted in this revision (for 15th-17th

August), namely RUN1 (with an increase of anthropogenic VOC emission by 50%) and RUN2 (with a decrease of anthropogenic VOC emission by 33%), to explore the sensitivity of simulated VOC and O₃ concentrations to anthropogenic VOC emissions. We found that 50% increases of anthropogenic VOC emission could lead to a 22% increase of urban VOC concentration, while the 33% emission decrease resulted in a 24% decrease of concentration (Table S2). It is worth noting that the concentration of O₃ stayed almost the same (because the O₃ production regime is NO_x-limit). We addressed that the uncertainties of VOC emission obviously affected the VOC concentrations; however, MEIC inventory is the most updated available emission for China so far, and quantifying its uncertainties can be done in future studies (possibly with satellite-based measurement of HCHO (Miller et al., 2008)).

We analyzed PM_{2.5} concentration and composition (sulfate, nitrate, ammonium, EC, organic matter) with the filter-base measurements. The model predicted PM_{2.5} concentration to be 94.6±28.2 μg m⁻³, slightly lower (NMB=-12%) than measured 107 μg m⁻³ averaged for the no-raining period, but didn't perform well in capturing temporal correlation (r=0.17). The simulated PM_{2.5} showed the similar compositions to the observation (Fig. S1b and S1c). Sulfate is the dominant constituent of both simulated (32%) and observed (37%) PM_{2.5}. High sulfate concentration was mainly attributed to the high SO₂ emission in the GZ basin as well as the humid weather conditions (Wang et al., 2014). The secondary constituent of observed PM_{2.5} is organic matter, which accounted for 16% of the total observed PM_{2.5}, close to the simulated result (14%). Secondary organic matter contributed half to total simulated organic matter, mainly due to the abundant precursor (i.e. VOCs) emissions and the high atmospheric oxidation capacity in summer.

4. Impacts of biogenic and anthropogenic sources on O₃ formation

In this section, we analyze the results from the four simulations (BASE, ANTH, BIO and NEITHER, Table 2) to characterize the fate of O₃ and its precursors in the GZ basin and to quantify the pure and synergistic impacts of anthropogenic and/or biogenic sources on summertime O₃ formation.

4.1 Base simulation of O₃

Firstly, we discuss the spatial and temporal characteristics of the simulated O₃ and the precursors (VOCs and NO_x) in the GZ basin in the BASE simulation.

Figure 4a shows spatial distribution of the simulated VOCs during the no-raining period, overlaid with the simulated wind vectors. The highest concentration (more than 50 ppb, with ethane being the dominant species) was in urban Xi'an and its downwind region (the southwest of urban Xi'an), due to anthropogenic activities. In addition, another high-value area (~30 ppb, with isoprene being the dominant species) was found in the Qinling Mountains, which was probably due to biogenic sources. To better understand the composition of VOCs, we analyzed some typical individual VOC species. Figure S2a shows the spatial distribution of xylenes, representing anthropogenic VOCs, and Fig. S3a and S4a show isoprene and monoterpenes, representing biogenic VOCs. The anthropogenic xylenes were mainly distributed in the GZ basin, while the high biogenic isoprene and monoterpene concentrations were found over the Qinling Mountains. These results explain the spatial feature of total VOCs and the dominant sources. Detailed discussion of source apportionment is given in Section 4.2

The spatial distribution of NO_x was slightly different (Fig. 5a). The highest concentrations of NO_x were in the GZ basin (average of 11.1 ppb), especially in urban Xi'an (averaged of 30.1 ppb), while among the Qinling Mountains, NO_x was low and dominated by biogenic sources.

PM, even though not directly involved in the formation pathways of O₃, influences the chemical equilibrium indirectly. In the daytime, NO₂ photolysis frequency ($J(\text{NO}_2)$) is determined by the solar radiation influenced by PM via scattering and absorption. Figure 6 shows the changes of $J(\text{NO}_2)$ (calculated by model track output `photor_no2`) with the participation of PM (concentration, 102 $\mu\text{g m}^{-3}$; aerosol optical depth (AOD) at 550 nm, 1.92; single scattering albedo (SSA) at 550 nm, 0.92) averaged for urban Xi'an. $J(\text{NO}_2)$ was reduced by 40-60%, most significantly in morning and evening rush hours. In the night time, PM_{2.5} can remove N₂O₅ from the NO_x cycle via heterogeneous reactions, as one of the major NO_x sinks in the atmosphere (Xue et al., 2014). Figure S5a shows the spatial feature of PM_{2.5}. The densest area was urban Xi'an (averaged for 102 $\mu\text{g m}^{-3}$) followed by the western part of the GZ basin. The spatial distribution of high-values of PM_{2.5} was similar to

that of NO_x , but covered a wider area mostly in the downwind region of urban Xi'an, which is expected due to longer lifetime of aerosols compared with NO_x and the time required for secondary aerosol formation, thus further dispersion.

The typical diurnal variation of O_3 (Fig. 7b) demonstrates there are higher concentrations in the afternoon and lower at night. For better understanding of O_3 concentration characteristics and source/sink mechanisms, we discussed two different time scales: 1) O_3 peak time (14:00-18:00) (Fig. 8) and 2) O_3 24-hour average (Fig. 9). During the peak time, simulated near-surface O_3 was high in the GZ basin, with averaged concentration of 75 ppb. In the downwind region of high NO_x and VOCs in the west of urban Xi'an, the concentration reached up to 110 ppb. We employed the ratio of $\text{H}_2\text{O}_2/\text{HNO}_3$ to investigate the chemistry regime of O_3 formation (Sillman 1995; Wang et al., 2017). If the ratio is greater than 0.5, the O_3 production regime is considered NO_x -controlled, otherwise VOC-controlled if the ratio less than 0.3. The range between 0.3 and 0.5 is defined as the transition regime from NO_x - to VOC-controlled, indicating the competition of both NO_x and VOCs in O_3 production. Figure 10a shows the spatial distribution of the simulated $\text{H}_2\text{O}_2/\text{HNO}_3$ ratio during the O_3 peak time. The west and southeast of the GZ basin were right in the transition regime with a complicated O_3 production mechanism sensitive to both NO_x and VOCs. Most of the rest of the simulation region was VOC-controlled, excluding the Yuncheng and Hejing cities in the neighboring Shanxi provinces.

On the 24h average scale, the spatial distribution of O_3 presented a different picture (Fig. 9). The original high-value area during the peak time in the GZ city cluster shifted to low-value region due to the consumption of O_3 by abundant NO_x emissions. At night time, the titration effect of freshly emitted NO dominates, and the O_3 concentration tends to drop to a lower level. The high value of 24h averaged O_3 converged in the south and northwest outside of the GZ Basin. Those areas have elevated O_3 due to high daytime production, similar to the nearby zone of peak O_3 , but also have lower emissions of NO resulting in lower loss of O_3 .

4.2 Pure impact of biogenic or anthropogenic sources

Using the FSA method, we evaluated the pure contribution of anthropogenic or

biogenic sources to the summertime O₃ formation in the GZ basin. In the scenario of pure contribution of anthropogenic emissions, the VOC concentrations were mostly distributed over the GZ city cluster (8.0 ppb), especially in urban Xi'an (26.4 ppb) (Fig. 4c). In the scenario of pure contribution of biogenic emissions, the VOCs were widely dispersed over the Qinling Mountains (Fig. 4d), with a calculated 9.9 ppb for the GZ basin and 12.4 ppb for urban Xi'an. NO_x concentration has the similar pattern as VOCs in the scenario of pure contribution of anthropogenic emissions, with averaged concentrations of 11.0 ppb for the GZ basin and 30.3 ppb for urban Xi'an (Fig. 5c). However, in the GZ basin and urban Xi'an, biogenic sources contributed less than 0.2 ppb to NO_x concentration (Fig. 5d). In the scenario of pure contribution of anthropogenic emissions, PM_{2.5} spread over a wider area (Fig. S5c), due to the time required for secondary aerosol formation. In the scenario of pure contribution of biogenic emissions, PM_{2.5} was mostly distributed among the Qinling Mountains (Fig. S5d), but the concentration was lower by one order of magnitude (Table 4, Fig. S6).

In the scenario of pure contribution of anthropogenic emissions, daily peak O₃ accumulated in the downwind region in the center and western GZ due to high VOCs and NO_x concentrations. Daily peak O₃ concentrations reached 22.6 ppb for GZ and 19.1 ppb for urban Xi'an (Fig. 8c). Lower daily peak O₃ concentration was found outside of GZ basin where less anthropogenic VOCs and NO_x was emitted. In contrast, daily peak O₃ was negligible (less than 3 ppb) in the scenario of pure contribution of biogenic emissions (Fig. 8d) due to the low NO_x emissions. However, the distribution of 24h averaged O₃ was different from daily peak O₃. 24h averaged O₃ concentration in the scenario of pure contribution of anthropogenic emissions was more diluted in the GZ city cluster than for surrounding areas (Fig. 9c). Due to the abundant NO emission and its titration effect on O₃, the pure effect of anthropogenic sources was negative, calculated to be -2.2 ppb in urban Xi'an.

4.3 Synergistic impact of the interaction between biogenic and anthropogenic sources

The synergistic impact on O₃ formation includes the interactions between anthropogenic and biogenic sources. In other word, it reflects the potential production trend of either "O₃-promoted" or "O₃-suppressed" under the natural coexistence of all

emission sources. In the cases of NO_x , VOCs and $\text{PM}_{2.5}$, the synergistic impacts contributed less than $\pm 3\%$ of total concentrations (Fig. 4b, 5b, S5b, S6, and Table 4). However, the synergistic impact on O_3 played a remarkable role showing positive impacts for both daily peak (Fig. 8b) and 24h averaged O_3 (Fig. 9b). It means that the mixed state of anthropogenic and biogenic sources potentially enhanced the O_3 production more than each single source. To make it more specific, we started the discussion from the result of ANTH simulation without the biogenic sources (Table 2). Figure 10b shows the O_3 production regime in the ANTH simulation. VOC-controlled O_3 production regime covered the west of urban Xi'an and the southeast of the GZ basin. In the rest of the GZ basin and the neighboring Shanxi provinces, the O_3 production was in the transition regime, controlled by both NO_x and VOC. NO_x -controlled O_3 production regime dominated the rest of the region. After we included biogenic VOC emissions in the simulation, the O_3 concentration was significantly enhanced in the VOC-controlled regions, and partly enhanced in the mix-controlled region. However, in the VOC-controlled region, the synergistic impact contributed little.

The synergistic impact is of great importance, approximately the same magnitude as the impact from pure contributions of anthropogenic sources. The synergistic impact contributed daily peak O_3 concentrations of 10.5 ppb for the GZ basin and 14.3 ppb for urban Xi'an, while the pure anthropogenic impact contributed 22.6 ppb for GZ basin and 19.1 ppb for urban Xi'an. However, the extent was $\sim 50\%$ smaller on the 24h averaged scale, but still increased O_3 concentration by 5.8 ppb for the GZ basin and 6.8 ppb for urban Xi'an. Figure 7 shows the diurnal variation of the observed and simulated O_3 concentration at Xi'an Jiaotong University, as well as the tested contributing components. Transport dominated O_3 , constantly contributing 30-40 ppb as background. The impact of pure anthropogenic sources was positive on O_3 production during 13:00-19:00 but negative during the rest of the time, and the impact of pure biogenic sources was negligible. Synergistic impact of both anthropogenic and biogenic sources resulted in a positive contribution during 10:00-21:00, comparable to the impact of pure anthropogenic sources.

It is worth noting that the biogenic contribution to $\text{PM}_{2.5}$ is not obvious (less than 3%) in GZ basin, which might be different from some other regions (e.g. Fu et al., 2012; Li et al., 2013). The main reasons are that 1) organic matter, the most important

biogenic PM_{2.5} component, only accounted for 14-16% of PM_{2.5} in GZ basin in August; 2) Undeniably, uncertainties still exist in organic matter simulations in the model.

5 5. Conclusions

The GZ basin is a representative region in the northwest of China, suffering serious air pollution in recent years. Geographically, the GZ basin borders the northern foot of the Qinling Mountains. For this reason, in addition to the anthropogenic emissions from metropolitan areas, biogenic emissions are of great importance in the region, especially in warm season with active photochemistry. In this study, we used the WRF-Chem model to simulate O₃ in the GZ basin and compared the results to near-surface measurements, with the aim of quantifying the pure and synergistic impacts of anthropogenic and/or biogenic sources on summertime O₃ formation. The simulation was driven by the best currently available inventory of anthropogenic emissions and online calculated biogenic emissions. Near-surface measurements were captured from 6 surface sites among the Qinling Mountains for biogenic VOCs and one 100-m-high site in the Xi'an city for air quality (NO_x, VOCs, O₃ and PM_{2.5}).

Our model successfully reproduced the observed air quality and meteorological parameters. The biogenic VOCs simulation showed a reasonable agreement. Our model also well-reproduced the magnitudes and variations of O₃, NO_x and PM_{2.5} concentrations excluding rainy days, with normalized mean bias less than ±21%.

We further conducted three scenario simulations to explore the pure and synergistic impacts of anthropogenic and/or biogenic sources on O₃ and the precursors, by using the factor separation approach (FSA). The results concluded that, for the precursors, pure impact of anthropogenic source contributed 99% of NO_x, 80% of PM_{2.5}, and 33% of VOCs in the GZ basin, and pure impact of biogenic source contributed 40% of VOCs but only 1-5% of PM_{2.5} and NO_x. Meanwhile, synergistic impacts from the combination of anthropogenic and biogenic sources did not bring significant changes on NO_x, VOCs and PM_{2.5} (less than ±4%). In the case of daily peak O₃, the pure impact of anthropogenic source remained the dominant contributor (19.1 ppb for urban Xi'an), even after anthropogenic particles reduced the NO₂

5 photolysis by up to 60%. The abundant biogenic VOCs from the nearby forests promoted the O₃ formation by interaction with anthropogenic NO_x, contributing 14.4 ppb to O₃ in urban Xi'an. This synergistic impact presented a positive contribution to O₃ production throughout the day and the positive effect was much more prominent during 12:00-19:00.

10 O₃ pollution in China has been raising increasing concerns in recent years. Some scientists hold the view that excessive concentration of PM_{2.5} suppressed the formation of O₃ in the past, hiding the problem temporally. However, with the effective control of PM_{2.5}, O₃ pollution is manifested. The phenomenon can also be demonstrated by the government control action during G20 summit (The Group of
15 Twenty Finance Ministers and Central Bank Governors) in Hangzhou in 2016. The concentration of PM_{2.5} was depressed sharply under the strict emission control, but O₃ concentration was even higher than usual. Better understanding of O₃ pollution sources/sinks and formation mechanisms in high PM_{2.5} exposed area in China will benefit and guide the implementation of PM_{2.5}/O₃ cooperative control. Our results suggest that, in big cities geographically close to forest, O₃ pollution can be enhanced by the synergistic impact from the combination of biogenic and anthropogenic sources. The synergistic contribution of each single source to O₃ formation cannot be neglected when making pollution control strategies.

20

Acknowledgments

25 This work was supported by the National Natural Science Foundation of China (41705128), Opening Project of State Key Laboratory of Loess and Quaternary Geology (SKLLQG1709), and Opening Project of Shanghai Key Laboratory of Atmospheric Particle Pollution and Prevention (LAP³) (FDLAP17003).

Reference

30 Binkowski, F.S., and Roselle, S.J.: Models-3 community multiscale air quality

- (CMAQ) model aerosol component-1. Model description, *J. Geophys. Res.*, 108, 4183, doi:10.1029/2001jd001409, 2003.
- 5 Bossioli, E., Tombrou, M., Karali, A., Dandou, A., Paronis, D., and Sofiev, M.: Ozone production from the interaction of wildfire and biogenic emissions: a case study in Russia during spring 2006, *Atmos. Chem. Phys.*, 12, 7931-7953, doi:10.5194/acp-12-7931-2012, 2012.
- 10 Brauer, M., Freedman, G., Frostad, J., van Donkelaar, A., Martin, R.V., Dentener, F., van Dingenen, R., Estep, K., Amini, H., Apte, J.S., Balakrishnan, K., Barregard, L., Broday, D., Feigin, V., Ghosh, S., Hopke, P.K., Knibbs, L.D., Kokubo, Y., Liu, Y., Ma, S., Morawska, L., Texcalac Sangrador, J. L., Shaddick, G., Anderson, H. R., Vos, T., Forouzanfar, M. H., Burnett, R.T., and Cohen, A.: Ambient Air Pollution Exposure Estimation for the Global Burden of Disease 2013, *Environ. Sci. Technol.*, 50, 79-88, doi:10.1021/acs.est.5b03709, 2016.
- 15 Carlo, P.D., Brune, W.H., Martinez, M., Harder, H., Lesher, R., Ren, X., Thornberry, T., Carroll, M. A., Young, V., and Shepson, P. B.: Missing OH Reactivity in a Forest: Evidence for Unknown Reactive Biogenic VOCs, *Science*, 304, 722-725, doi: 10.1126/science.1094392, 2004.
- 20 Carter W.P.L. and Atkinson R.: Development and evaluation of a detailed mechanism for the atmospheric reactions of isoprene and NO_x. *Int. J. Chem. Kinet.*, 28, 497-530, 1996.
- Chow, J.C., Watson, J.G., Chen, L.W.A., Chang, M.C.O., Robinson, N.F., Trimble, D., and Kohl, S.: The IMPROVE-A temperature protocol for thermal/optical carbon analysis: maintaining consistency with a long-term database, *J. Air. Waster. Manage.*, 57, 1014-1023, doi:10.3155/1047-3289.57.9.1014, 2007.
- 25 Curci, G., Beekmann, M., Vautard, R., Smiatek, G., Steinbrecher, R., Theloke, J., and Friedrich, R.: Modelling study of the impact of isoprene and terpene biogenic emissions on European ozone levels, *Atmos. Environ.*, 43, 1444-1455, doi:10.1016/j.atmosenv.2008.02.070, 2009.
- 30 Ehhalt, D.H., and Rohrer, F.: Dependence of the OH concentration on solar UV, *J. Geophys. Res.*, 105, 3565-3571, 2000.
- Emmons, L.K., Walters, S., Hess, P.G., Lamarque, J.F., Pfister, G.G., Fillmore, D., Granier, C., Guenther, A., Kinnison, D., Laepple, T., Orlando, J., Tie, X., Tyndall, G., Wiedinmyer, C., Baughcum, S.L., and Kloster, S.: Description and evaluation of the Model for Ozone and Related chemical Tracers, version 4 (MOZART-4), *Geosci. Model Dev.*, 3, 43-67, doi:10.5194/gmd-3-43-2010, 2010.
- 35 Feng, T., Bei, N., Huang, R.J., Cao, J., Zhang, Q., Zhou, W., Tie, X., Liu, S., Zhang, T., Su, X., Lei, W., Molina, L. T., and Li, G.: Summertime ozone formation in Xi'an and surrounding areas, China, *Atmos. Chem. Phys.*, 16, 4323-4342, doi:10.5194/acp-16-4323-2016, 2016.
- 40 Feng, Z., Hu, E., Wang, X., Jiang, L., and Liu, X.: Ground-level O₃ pollution and its impacts on food crops in China: A review, *Environ. Pollut.*, 199, 42-48, doi:10.1016/j.envpol.2015.01.016, 2015.
- Fiore, A.M., Horowitz, L.W., Purves, D.W., Levy, H., Evans, M.J., Wang, Y.X., Li, Q.B., and Yantosca, R.M.: Evaluating the contribution of changes in isoprene

emissions to surface ozone trends over the eastern United States, *J. Geophys. Res.*, 110, doi:10.1029/2004jd005485, 2005.

- 5 Fiore, A.M., Levy, H. II, and Jaffe, D.A.: North American isoprene influence on intercontinental ozone pollution, *Atmos. Chem. Phys.*, 11, 1697-1710, doi:10.5194/acp-11-1697-2011, 2011.
- 10 Fisher, J.A., Jacob, D.J., Travis, K.R., Kim, P.S., Marais, E.A., Miller, C.C., Yu, K., Zhu, L., Yantosca, R.M., and Sulprizio, M.P.: Organic nitrate chemistry and its implications for nitrogen budgets in an isoprene- and monoterpene-rich atmosphere: constraints from aircraft (SEAC4RS) and ground-based (SOAS) observations in the Southeast US, *Atmos. Chem. Phys.*, 16, 1-38, doi: 10.5194/acp-16-5969-2016, 2016.
- 15 Fu, T.M., Cao, J.J., Zhang, X.Y., Lee, S.C., Zhang, Q., Han, Y.M., Qu, W.J., Han, Z., Zhang, R., Wang, Y.X., Chen, D., and Henze, D. K.: Carbonaceous aerosols in China: top-down constraints on primary sources and estimation of secondary contribution, *Atmos. Chem. Phys.*, 12, 2725-2746, doi:10.5194/acp-12-2725-2012, 2012.
- Fu, T.-M., Zheng, Y., Paulot, F., Mao, J., and Yantosca, R.M.: Positive but variable sensitivity of August surface ozone to large-scale warming in the southeast United States, *Nat. Clim. Change*, 5, 454-458, doi:10.1038/nclimate2567, 2015.
- 20 Fu, Y., and Liao, H.: Simulation of the interannual variations of biogenic emissions of volatile organic compounds in China: impacts on tropospheric ozone and secondary organic aerosol, *Atmos. Environ.*, 59, 170-185, doi:10.1016/j.atmosenv.2012.05.053, 2012.
- 25 Fu, Y., and Liao, H.: Impacts of land use and land cover changes on biogenic emissions of volatile organic compounds in China from the late 1980s to the mid-2000s: implications for tropospheric ozone and secondary organic aerosol, *Tellus B*, 66, doi:10.3402/tellusb.v66.24987, 2014.
- 30 Geng, F., Tie, X., Guenther, A., Li, G., Cao, J., and Harley, P.: Effect of isoprene emissions from major forests on ozone formation in the city of Shanghai, China, *Atmos. Chem. Phys.*, 11, doi:10449-10459, 10.5194/acp-11-10449-2011, 2011.
- Geng, G., Zhang, Q., Martin, R. V., Lin, J., Huo, H., Zheng, B., Wang, S., and He, K.: Impact of spatial proxies on the representation of bottom-up emission inventories: A satellite-based analysis, *Atmos. Chem. Phys.*, 17, 4131-4145, doi:10.5194/acp-17-4131-2017, 2017.
- 35 Grell, G.A., Peckham, S.E., Schmitz, R., McKeen, S.A., Frost, G., Skamarock, W.C., and Eder, B.: Fully coupled "online" chemistry within the WRF model, *Atmos. Environ.*, 39, 6957-6975, doi:10.1016/j.atmosenv.2005.04.027, 2005.
- 40 Guenther, A., Hewitt, C.N., Erickson, D., Fall, R., Geron, C., Graedel, T., Harley, P., Klinger, L., Lerdau, M., McKay, W.A., Pierce, T., Scholes, B., Steinbrecher, R., Tallamraju, R., Taylor, J., and Zimmerman, P.: a global-model of natural volatile organic-compound emissions, *J. Geophys. Res.*, 100, 8873-8892, doi:10.1029/94jd02950, 1995.
- Guenther, A., Karl, T., Harley, P., Wiedinmyer, C., Palmer, P.I., and Geron, C.: Estimates of global terrestrial isoprene emissions using MEGAN (Model of

- Emissions of Gases and Aerosols from Nature), *Atmos. Chem. Phys.*, 6, 3181-3210, doi:10.5194/acp-6-3181-2006, 2006.
- Horowitz, L. W., Fiore, A.M., Milly, G.P., Cohen, R.C., Perring, A., Wooldridge, P.J., Hess, P.G., Emmons, L.K., and Lamarque J.F.: Observational constraints on the chemistry of isoprene nitrates over the eastern United States, *J. Geophys. Res.*, 112, D12S08, doi:10.1029/2006JD007747, 2007.
- Hu, J., Chen, J., Ying, Q., and Zhang, H.: One-Year Simulation of Ozone and Particulate Matter in China Using WRF/CMAQ Modeling System, *Atmos. Chem. Phys.*, 16, 10333-10350, doi:10.5194/acp-16-10333-2016, 2016.
- Hudman, R.C., Murray, L.T., Jacob, D.J., Turquety, S., Wu, S., Millet, D.B., Avery, M., Goldstein, A.H., and Holloway, J.: North American influence on tropospheric ozone and the effects of recent emission reductions: Constraints from ICARTT observations, *J. Geophys. Res.*, 114, D07302, doi:10.1029/2008JD010126, 2009.
- Im, U., Poupkou, A., Incecik, S., Markakis, K., Kindap, T., Unal, A., Melas, D., Yenigun, O., Topcu, S., Odman, M.T., Tayanc, M., and Guler, M.: The impact of anthropogenic and biogenic emissions on surface ozone concentrations in Istanbul, *Sci. Total Environ.*, 409, 1255-1265, doi:10.1016/j.scitotenv.2010.12.026, 2011.
- IPCC: Working group I contribution to the IPCC Fifth Assessment Report Climate Change 2013: the Physical Science Basis, Cambridge University Press, Cambridge, New York, 2013
- Jiang, H., Liao, H., Pye, H.O.T., Wu, S., Mickley, L.J., Seinfeld, J.H., and Zhang, X.Y.: Projected effect of 2000-2050 changes in climate and emissions on aerosol levels in China and associated transboundary transport, *Atmos. Chem. Phys.*, 13, 7937-7960, doi:10.5194/acp-13-7937-2013, 2013.
- Kota, S. H., Schade, G., Estes, M., Boyer, D., and Ying, Q.: Evaluation of MEGAN predicted biogenic isoprene emissions at urban locations in Southeast Texas, *Atmospheric Environment*, 110, 54-64, 10.1016/j.atmosenv.2015.03.027, 2015.
- Kurokawa, J., Ohara, T., Morikawa, T., Hanayama, S., Janssens-Maenhout, G., Fukui, T., Kawashima, K., and Akimoto, H.: Emissions of air pollutants and greenhouse gases over Asian regions during 2000-2008: Regional Emission inventory in ASia (REAS) version 2, *Atmos. Chem. Phys.*, 13, 11019-11058, doi:10.5194/acp-13-11019-2013, 2013.
- Lee, K.-Y., Kwak, K.-H., Ryu, Y.-H., Lee, S.-H., and Baik, J.-J.: Impacts of biogenic isoprene emission on ozone air quality in the Seoul metropolitan area, *Atmos. Environ.*, 96, 209-219, doi:10.1016/j.atmosenv.2014.07.036, 2014.
- Lei, Y., Zhang, Q., He, K. B., and Streets, D. G.: Primary anthropogenic aerosol emission trends for China, 1990-2005, *Atmos. Chem. Phys.*, 11, 931-954, doi:10.5194/acp-11-931-2011, 2011.
- Li, G., Lei, W., Zavala, M., and Volkamer, R.: Impacts of HONO sources on the photochemistry in Mexico City during the MCMA-2006/MILAGO Campaign, *Atmos. Chem. Phys.*, 10, 14, 6551-6567, 10.5194/acp-10-6551-2010, 2010.
- Li, G., Bei, N., Tie, X., and Molina, L. T.: Aerosol effects on the photochemistry in

Mexico City during MCMA-2006/MILAGRO campaign, *Atmos. Chem. Phys.*, 11, 5169-5182, doi:10.5194/acp-11-5169-2011, 2011.

- 5 Li, L.Y., and Xie, S. D.: Historical variations of biogenic volatile organic compound emission inventories in China, 1981-2003, *Atmos. Environ.*, 95, 185-196, doi:10.1016/j.atmosenv.2014.06.033, 2014.
- Li, M., Zhang, Q., Kurokawa, J.I., Woo, J. H., He, K., Lu, Z., Ohara, T., Song, Y., Streets, D.G., Carmichael, G.R., Cheng, Y., Hong, C., Huo, H., Jiang, X., Kang, S., Liu, F., Su, H., and Zheng, B.: MIX: a mosaic Asian anthropogenic emission inventory under the international collaboration framework of the MICS-Asia and HTAP, *Atmos. Chem. Phys.*, 17, 935-963, doi:10.5194/acp-17-935-2017, 2017.
- 10 Li, N., Fu, T.-M., Cao, J., Lee, S., Huang, X.-F., He, L.-Y., Ho, K.-F., Fu, J. S., and Lam, Y.-F.: Sources of secondary organic aerosols in the Pearl River Delta region in fall: Contributions from the aqueous reactive uptake of dicarbonyls, *Atmos. Environ.*, 76, 200-207, doi:10.1016/j.atmosenv.2012.12.005, 2013.
- 15 Lin, J.-T., Patten, K.O., Hayhoe, K., Liang, X.-Z., and Wuebbles, D.J.: Effects of future climate and biogenic emissions changes on surface ozone over the United States and China, *J. Appl. Meteorol. Clim.*, 47, 1888-1909, doi:10.1175/2007jamc1681.1, 2008.
- Liu, Q., Lam, K.S., Jiang, F., Wang, T.J., Xie, M., Zhuang, B.L., and Jiang, X.Y.: A numerical study of the impact of climate and emission changes on surface ozone over South China in autumn time in 2000-2050, *Atmos. Environ.*, 76, 227-237, doi:10.1016/j.atmosenv.2013.01.030, 2013.
- 20 Millet, D.B., Jacob, D.J., Boersma, K.F., Fu, T.M., Kurosu, T.P., Chance, K., Heald, C.L., and Guenther, A.: Spatial distribution of isoprene emissions from North America derived from formaldehyde column measurements by the OMI satellite sensor, *J. Geophys. Res.*, 113, D02307, doi:10.1029/2007JD008950, 2008.
- 25 Paulot, F., Crounse, J.D., Kjaergaard, H.G., Kroll, J.H., Seinfeld, J.H., and Wennberg, P.O.: Isoprene photooxidation: New insights into the production of acids and organic nitrates, *Atmos. Chem. Phys.*, 9(4), 1479-1501, doi:10.5194/acp-9-1479-2009, 2009a.
- 30 Paulot, F., Crounse, J.D., Kjaergaard, H.G., Kurten, A., St Clair, J.M., Seinfeld, J.H., and Wennberg, P.O.: Unexpected epoxide formation in the gas-phase photooxidation of isoprene, *Science*, 325(5941), 730-733, doi:10.1126/science.1172910, 2009b.
- 35 Paulot, F., Henze, D.K., and Wennberg, P.O.: Impact of the isoprene photochemical cascade on tropical ozone, *Atmos. Chem. Phys.*, 12(3), 1307-1325, doi:10.5194/acp-12-1307-2012, 2012.
- 40 Qu, Y., An, J., and Li, J.: Synergistic impacts of anthropogenic and biogenic emissions on summer surface O₃ in East Asia, *J. Environ. Sci.*, 25, 520-530, doi:10.1016/s1001-0742(12)60069-2, 2013.
- Qu, Y., An, J., Li, J., Chen, Y., Li, Y., Liu, X., and Hu, M.: Effects of NO_x and VOCs from five emission sources on summer surface O₃ over the Beijing-Tianjin-Hebei region, *Adv. Atmos. Sci.*, 31, 787-800, doi:10.1007/s00376-013-3132-x, 2014.

- Rohrer, F., and Berresheim, H.: Strong correlation between levels of tropospheric hydroxyl radicals and solar ultraviolet radiation, *Nature*, 442, 184, doi:10.1038/nature04924, 2006.
- 5 Sillman, S.: The use of NO_y, H₂O₂, and HNO₃ as indicators for ozone-NO_x-hydrocarbon sensitivity in urban locations, *J. Geophys. Res.*, 100, 14175-14188, doi:10.1029/94jd02953, 1995.
- Skamarock, W. C., Klemp, J.B., Dudhia, J., Gill, D.O., Barker, D.M., Duda, M.G., Huang, X.Y., Wang, W., and Powers, J.G.: A Description of the Advanced Research WRF Version 3, Technical Report, National Center for Atmospheric Research, TN-475,+STR, 2008.
- 10 Squire, O.J., Archibald, A.T., Abraham, N.L., Beerling, D.J., Hewitt, C.N., Lathiere, J., Pike, R.C., Telford, P.J., and Pyle, J.A.: Influence of future climate and cropland expansion on isoprene emissions and tropospheric ozone, *Atmos. Chem. Phys.*, 14, 1011-1024, doi:10.5194/acp-14-1011-2014, 2014.
- 15 Stein, U., and Alpert, P.: Factor separation in numerical simulations, *J. Atmos. Sci.*, 50, 2107-2115, doi:10.1175/1520-0469(1993)050<2107:fsins>2.0.co;2, 1993.
- Stevenson, D.S., Young, P.J., Naik, V., Lamarque, J.F., Shindell, D.T., Voulgarakis, A., Skeie, R.B., Dalsoren, S.B., Myhre, G., Berntsen, T.K., Folberth, G.A., Rumbold, S.T., Collins, W.J., MacKenzie, I.A., Doherty, R.M., Zeng, G., van Noije, T.P.C., Strunk, A., Bergmann, D., Cameron-Smith, P., Plummer, D.A., Strode, S.A., Horowitz, L., Lee, Y.H., Szopa, S., Sudo, K., Nagashima, T., Josse, B., Cionni, I., Righi, M., Eyring, V., Conley, A., Bowman, K.W., Wild, O., and Archibald, A.: Tropospheric ozone changes, radiative forcing and attribution to emissions in the Atmospheric Chemistry and Climate Model Intercomparison Project (ACCMIP), *Atmos. Chem. Phys.*, 13, 3063-3085, doi:10.5194/acp-13-3063-2013, 2013.
- 20 Stockwell, W.R., Middleton, P., Chang, J.S., and Tang, X.: The second generation regional acid deposition model chemical mechanism for regional air quality modeling, *J. Geophys. Res.*, 95, D10, 16343-16367, doi: 0148-0227/90/90JD-00461\$05.00, 1990.
- 30 Strong, J., Whyatt, J.D., Metcalfe, S.E., Derwent, R.G., and Hewitt, C.N.: Investigating the impacts of anthropogenic and biogenic VOC emissions and elevated temperatures during the 2003 ozone episode in the UK, *Atmos. Environ.*, 74, 393-401, doi:10.1016/j.atmosenv.2013.04.006, 2013.
- Tian, Y., Dickinson, R.E., Zhou, L., Myneni, R.B., Friedl, M., Schaaf, C.B., Carroll, M., Gao, F.: Land boundary conditions from MODIS data and consequences for the albedo of a climate model. *Geophys. Res. Lett.*, 31, L05504, doi: 10.1029/2003GL019104, 2004.
- 35 Tie, X.X., Madronich, S., Walters, S., Zhang, R.Y., Rasch, P., and Collins, W.: Effect of clouds on photolysis and oxidants in the troposphere, *J. Geophys. Res.*, 108, doi:10.1029/2003jd003659, 2003.
- 40 Travis, K.R., Jacob, D.J., Fisher, J.A., Kim, P.S., Marais, E.A., Zhu, L., Yu, K., Miller, C.C., Yantosca, R.M., Sulprizio, M.P., Thompson, A.M., Wennberg, P.O., Crouse, J.D., St Clair, J.M., Cohen, R.C., Laughner, J.L., Dibb, J.E., Hall, S.R., Ullmann, K., Wolfe, G.M., Pollack, I.B., Peischl, J., Neuman, J.A., and Zhou, X.:

Why do models overestimate surface ozone in the Southeast United States?
Atmos. Chem. Phys., 16, 13561-13577, doi:10.5194/acp-16-13561-2016, 2016.

- 5 Wagner, P., and Kuttler, W.: Biogenic and anthropogenic isoprene in the near-surface urban atmosphere-A case study in Essen, Germany, *Sci. Total Environ.*, 475, 104-115, doi:10.1016/j.scitotenv.2013.12.026, 2014.
- Wang, D., Hu, J., Xu, Y., Lv, D., Xie, X., Kleeman, M., Xing, J., Zhang, H., and Ying, Q.: Source contributions to primary and secondary inorganic particulate matter during a severe wintertime PM_{2.5} pollution episode in Xi'an, China, *Atmos. Environ.*, 97, 182-194, doi:10.1016/j.atmosenv.2014.08.020, 2014.
- 10 Wang, M., Sampson, P.D., Hu, J., Kleeman, M., Keller, J. P., Olives, C., Szpiro, A.A., Vedal, S., and Kaufman, J.D.: Combining Land-Use Regression and Chemical Transport Modeling in a Spatiotemporal Geostatistical Model for Ozone and PM_{2.5}, *Environ. Sci. Technol.*, 50, 5111-5118, doi:10.1021/acs.est.5b06001, 2016.
- 15 Wang, Q., Han, Z., Wang, T., and Zhang, R.: Impacts of biogenic emissions of VOC and NO_x on tropospheric ozone during summertime in eastern China, *Sci. Total Environ.*, 395, 41-49, doi:10.1016/j.scitotenv.2008.01.059, 2008.
- Wang, T., Xue, L., Brimblecombe, P., Yun, F.L., Li, L., and Zhang, L.: Ozone pollution in China: A review of concentrations, meteorological influences, 20 chemical precursors, and effects, *Sci. Total Environ.*, 575, 1582-1596, doi:10.1016/j.scitotenv.2016.10.081, 2017.
- Wang, X., Shen, Z., Cao, J., Zhang, L., Liu, L., Li, J., Liu, S., and Sun, Y.: Characteristics of surface ozone at an urban site of Xi'an in Northwest China, *J. Environ. Monitor.*, 14, 116-126, doi:10.1039/c1em10541h, 2012.
- 25 Wang, Y., Shen, L., Wu, S., Mickley, L., He, J., and Hao, J.: Sensitivity of surface ozone over China to 2000-2050 global changes of climate and emissions, *Atmos. Environ.*, 75, 374-382, doi:10.1016/j.atmosenv.2013.04.045, 2013.
- Wesely, M. L.: Parameterization of surface resistances to gaseous dry deposition in regional-scale numerical-models, *Atmos. Environ.*, 23, 1293-1304, 30 doi:10.1016/0004-6981(89)90153-4, 1989.
- World Health Organization (WHO): Air Quality Guidelines for particulate matter, ozone, nitrogen dioxide and sulfur dioxide. Global update, 2005.
- Wu, S., Mickley, L.J., Jacob, D.J., Logan, J.A., Yantosca, R.M., and Rind, D.: Why are there large differences between models in global budgets of tropospheric 35 ozone?, *J. Geophys. Res.*, 112, doi:10.1029/2006jd007801, 2007.
- Wu, S., Mickley, L.J., Leibensperger, E.M., Jacob, D.J., Rind, D., and Streets, D.G.: Effects of 2000-2050 global change on ozone air quality in the United States, *J. Geophys. Res.*, 113, doi:10.1029/2007jd008917, 2008.
- 40 Xu, Z., Wang, T., Xue, L. K., Louie, P. K. K., Luk, C. W. Y., Gao, J., Wang, S. L., Chai, F. H., and Wang, W. X.: Evaluating the uncertainties of thermal catalytic conversion in measuring atmospheric nitrogen dioxide at four differently polluted sites in China, *Atmos. Environ.*, 76, 221-226, doi: 10.1016/j.atmosenv.2012.09.043, 2013.

- Xue, L.K., Wang, T., Gao, J., Ding, A.J., Zhou, X.H., Blake, D.R., Wang, X.F., Saunders, S.M., Fan, S.J., Zuo, H.C., Zhang, Q.Z., and Wang, W.X.: Ground-level ozone in four Chinese cities: precursors, regional transport and heterogeneous processes, *Atmos. Chem. Phys.*, 14, 13175-13188, doi:10.5194/acp-14-13175-2014, 2014.
- 5
- Xue, Y., Ho, S., Huang, Y., Li, B., Wang, L., Dai, W., Cao, J., and Lee, S.: Source apportionment of VOCs and their impacts on surface ozone in an industry city of Baoji, Northwestern China, *Sci. Rep.*, 7, 9979, doi:10.1038/s41598-017-10631-4, 2017.
- 10
- Zare, A., Christensen, J. H., Irannejad, P., and Brandt, J.: Evaluation of two isoprene emission models for use in a long-range air pollution model, *Atmos Chem Phys*, 12, 7399-7412, 10.5194/acp-12-7399-2012, 2012.
- Zhang, Q., Streets, D. G., Carmichael, G. R., He, K. B., Huo, H., Kannari, A., Klimont, Z., Park, I. S., Reddy, S., Fu, J. S., Chen, D., Duan, L., Lei, Y., Wang, L. T., and Yao, Z. L.: Asian emissions in 2006 for the NASA INTEX-B mission, *Atmos. Chem. Phys.*, 9, 5131-5153, doi:10.5194/acp-9-5131-2009, 2009.
- 15
- Zhang, R., Cohan, A., Biazar, A.P., and Cohan, D.S.: Source apportionment of biogenic contributions to ozone formation over the United States, *Atmos. Environ.*, 164, 8-19, doi:10.1016/j.atmosenv.2017.05.044, 2017.
- 20
- Zhang, T., Cao, J.J., Chow, J.C., Shen, Z.X., Ho, K.F., Ho, S.S.H., Liu, S.X., Han, Y.M., Watson, J.G., and Wang, G.H.: Characterization and seasonal variations of levoglucosan in fine particulate matter in Xi'an, China, *J. Air Waste Manage.*, 64, 1317-1327, doi:10.1080/10962247.2014.944959, 2014.
- Zhao, Y., Nielsen, C. P., Lei, Y., McElroy, M. B., and Hao, J.: Quantifying the uncertainties of a bottom-up emission inventory of anthropogenic atmospheric pollutants in China, *Atmos. Chem. Phys.*, 11, 2295-2308, doi:10.5194/acp-11-2295-2011, 2011.
- 25
- Zhu, J., and Liao, H.: Future ozone air quality and radiative forcing over China owing to future changes in emissions under the Representative Concentration Pathways (RCPs), *J. Geophys. Res.*, 121, 1978-2001, doi:10.1002/2015JD023926, 2016.
- 30
- Zhu, J., Liao, H., Mao, Y., Yang, Y., and Jiang, H.: Interannual variation, decadal trend, and future change in ozone outflow from East Asia, *Atmos. Chem. Phys.*, 17, 1-37, doi:10.5194/acp-17-3729-2017, 2017.

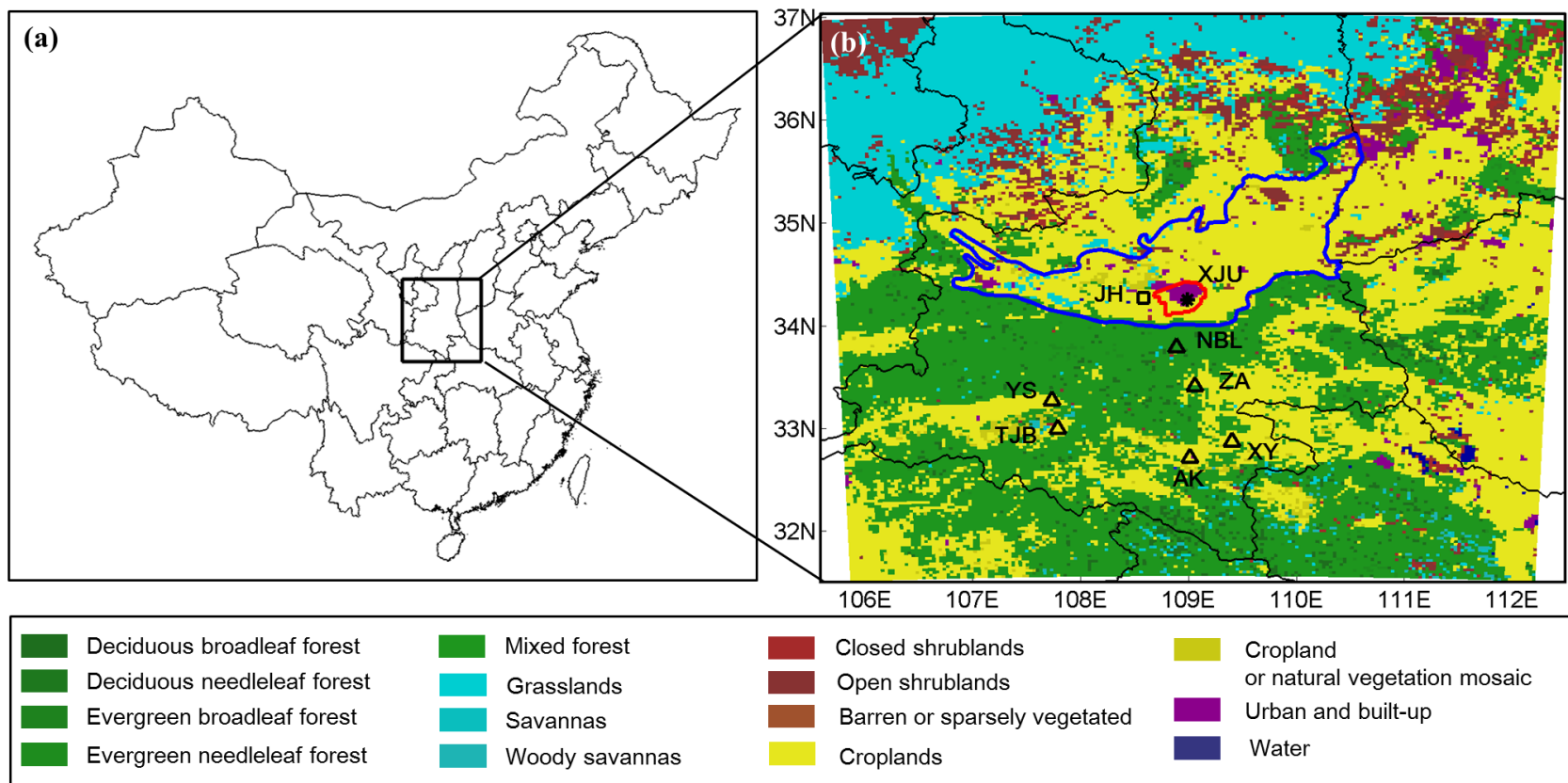


Figure 1. The simulation domain and the locations of six biogenic VOCs sites (triangles), one meteorological site (square) and one air quality site (snowflake). Underlain are land types from MODIS. The area of red line indicates the urban area of the Xi'an city. The area of blue line indicates the GZ basin.

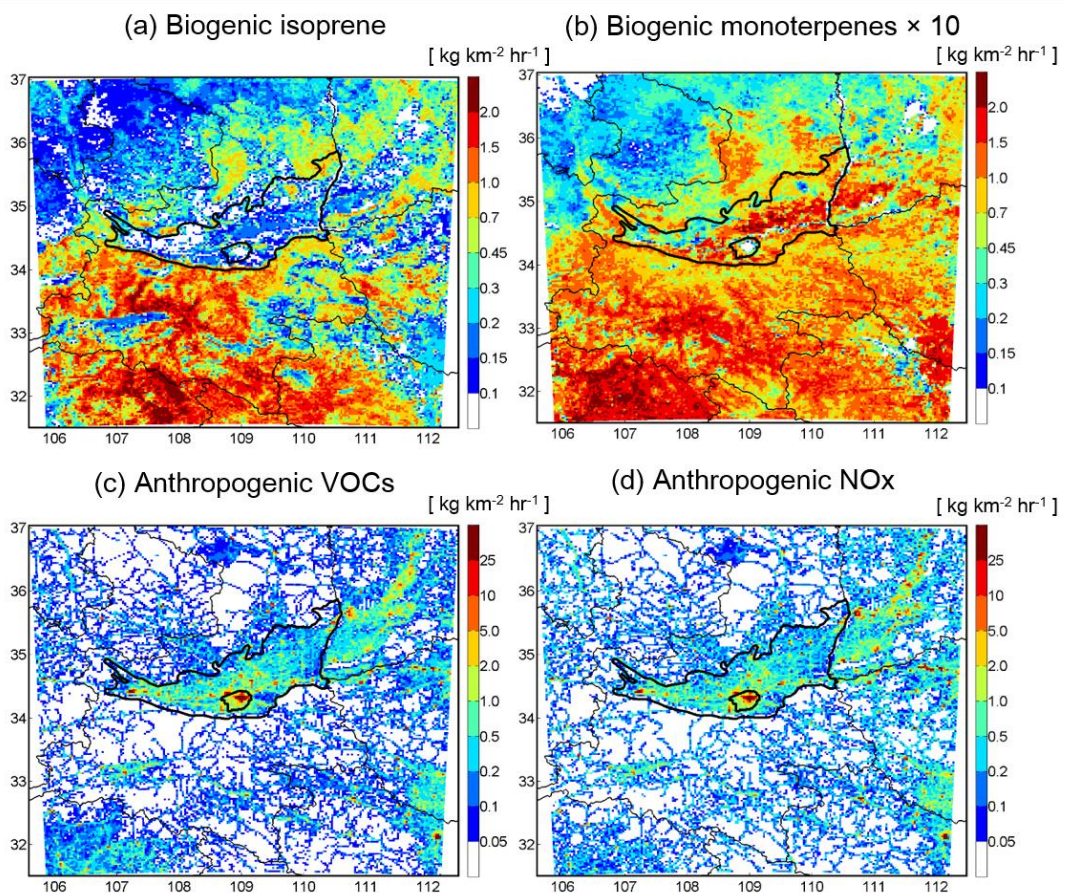


Figure 2. Monthly mean emissions of (a) biogenic isoprene, (b) biogenic monoterpenes, (c) anthropogenic VOCs and (d) anthropogenic NO_x in the GZ basin and surrounding areas in August 2011.

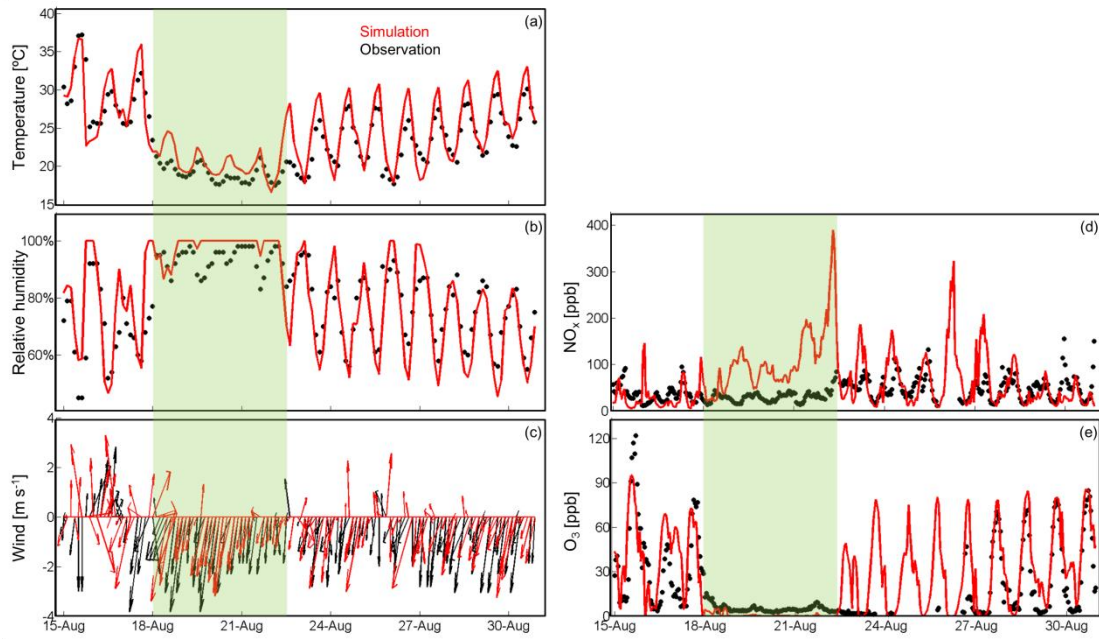


Figure 3. Observed (black) and simulated (red) temporal patterns of temperature (a), relative humidity (b) and wind (c) at the Jinghe site and NO_x (d) and O₃ (e) concentrations at Xi'an Jiaotong University during the period from 15th to 30th August 2011. The green shadow (18th -22nd August) indicates rainy days.

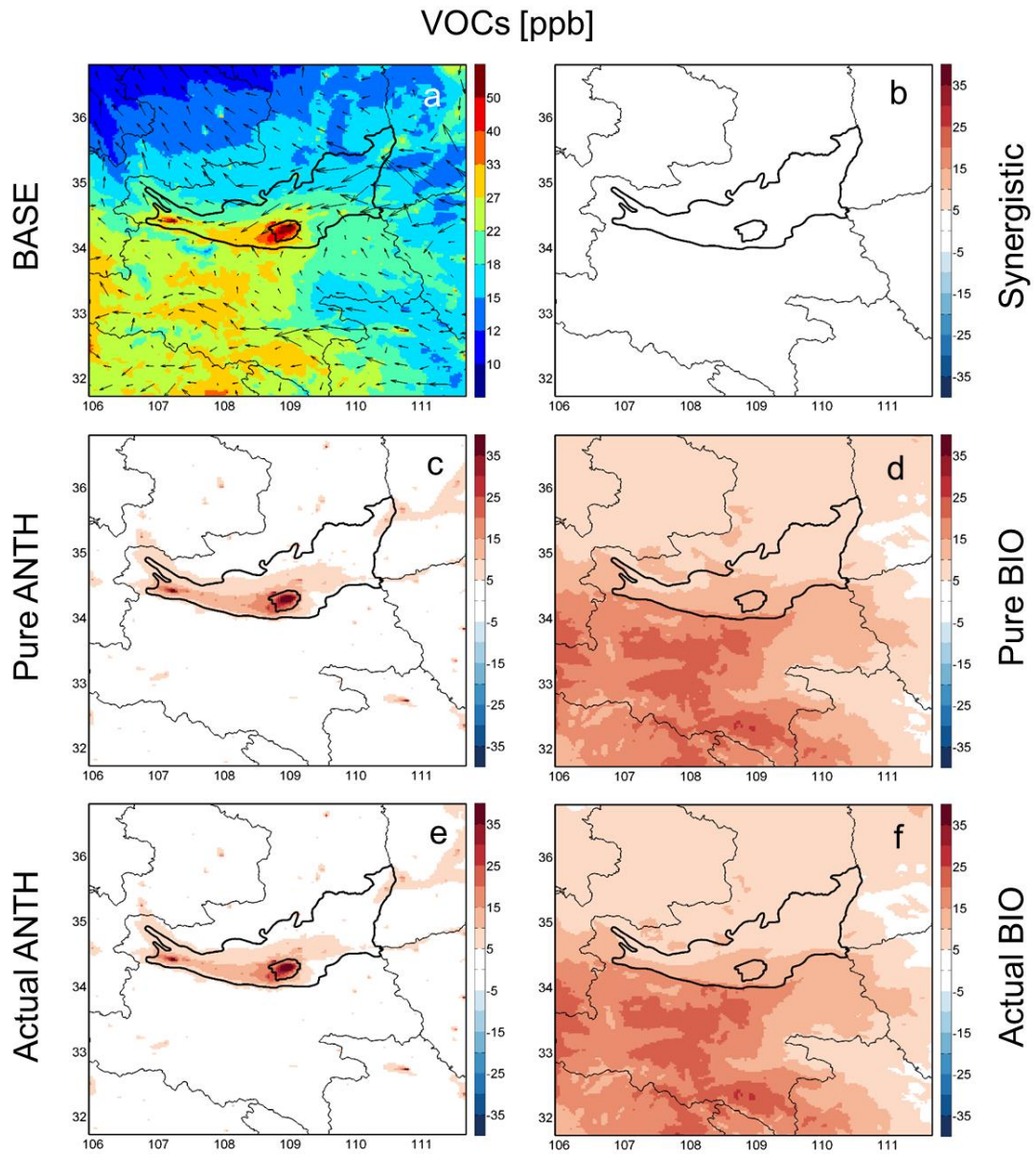


Figure 4. Spatial distributions of monthly mean concentrations of VOCs in August 2011. (a) is the result from the BASE simulation, overlaid with simulated wind vectors. (b)-(f) are simulated VOCs concentrations contributed from synergistic anthropogenic and biogenic, pure anthropogenic, pure biogenic, actual anthropogenic and actual biogenic sources, respectively.

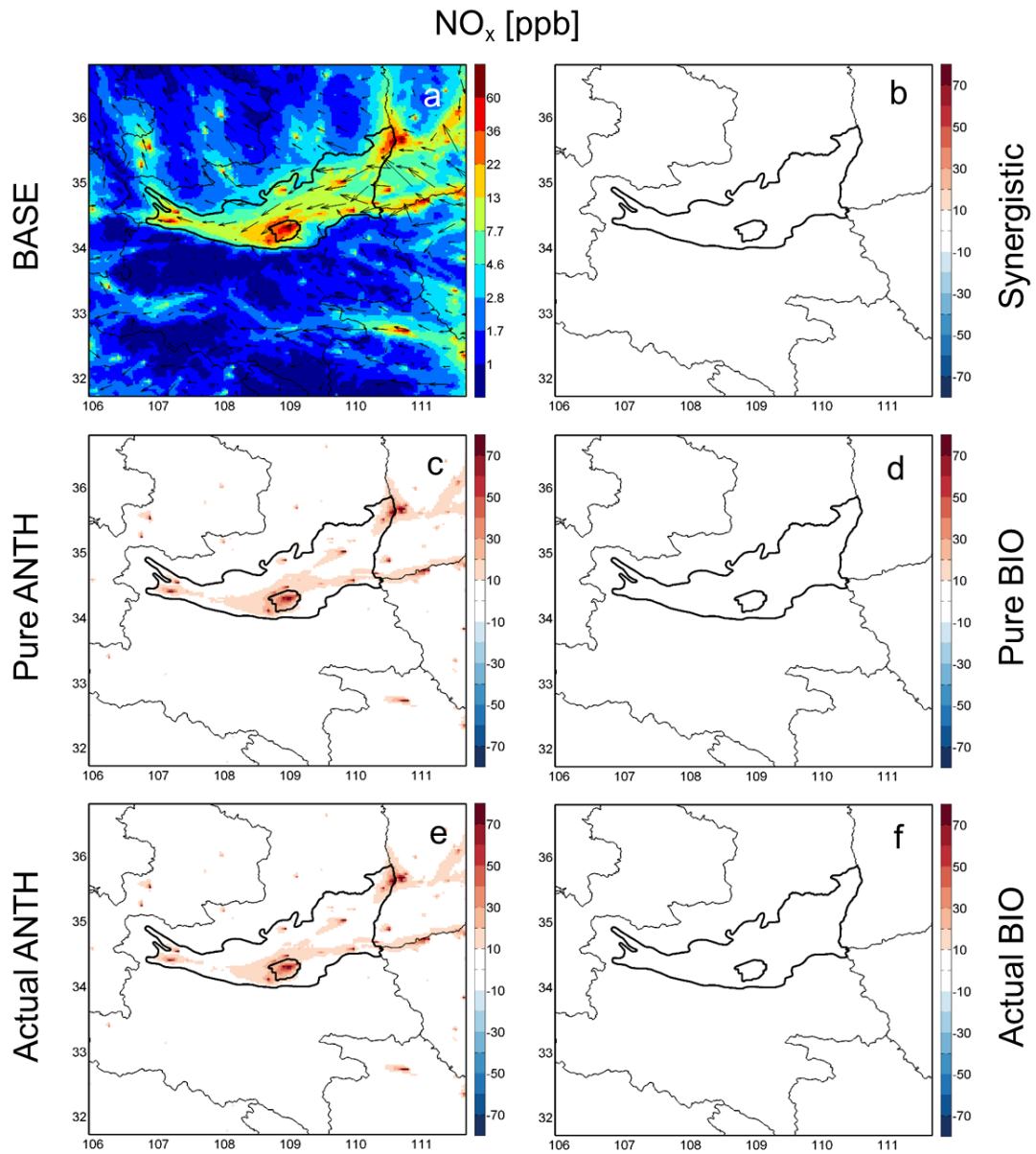


Figure 5. Spatial distributions of monthly mean concentrations of NO_x in August 2011. (a) is the result from the BASE simulation, overlaid with simulated wind vectors. (b)-(f) are simulated NO_x concentrations contributed from synergistic anthropogenic and biogenic, pure anthropogenic, pure biogenic, actual anthropogenic and actual biogenic sources, respectively.

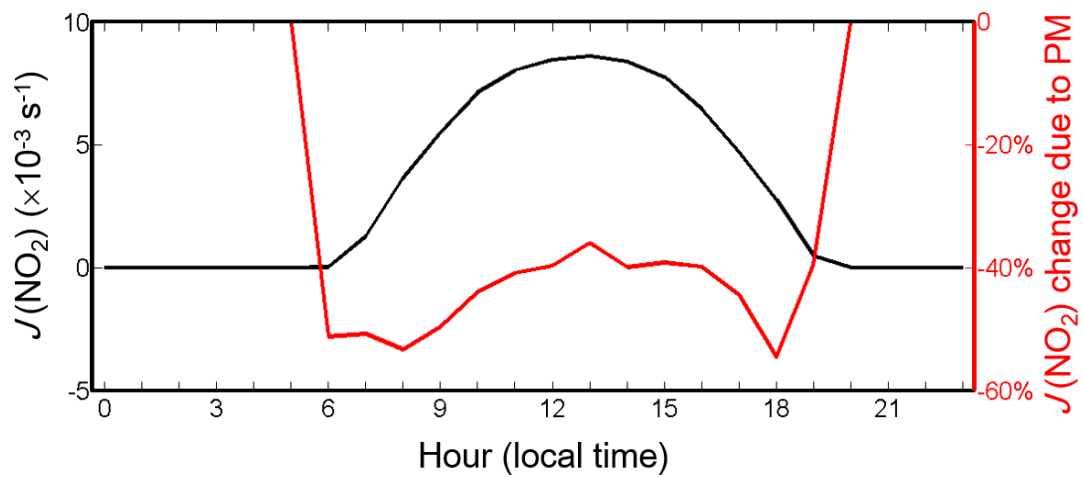


Figure 6. Diurnal variations of $J(\text{NO}_2)$ (black) and the changes in $J(\text{NO}_2)$ (red) averaged in urban Xi'an due to PM effects in August 2011.

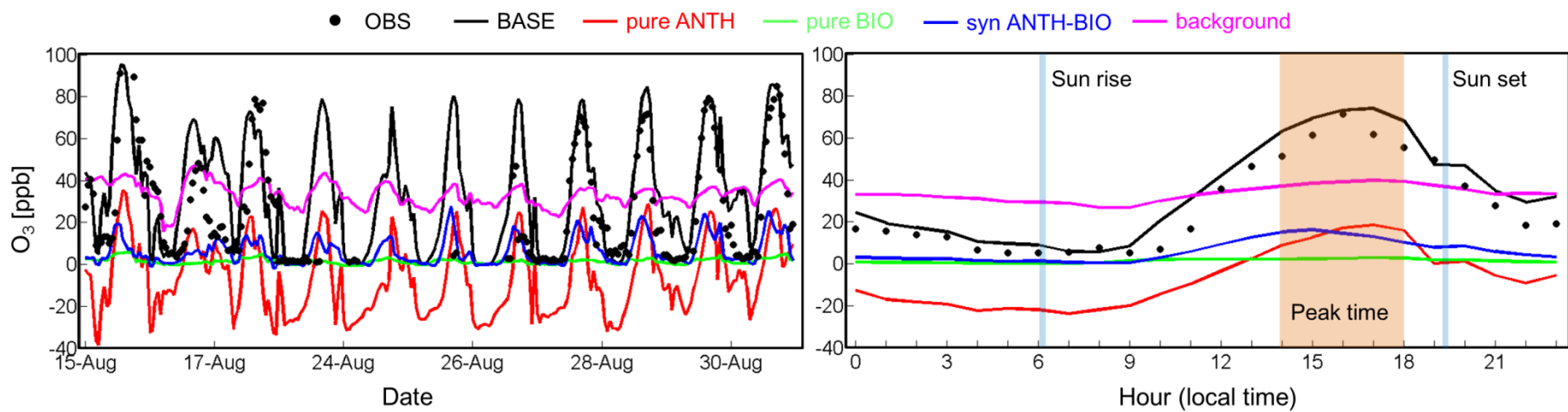


Figure 7. Temporal patterns of the simulated O₃ concentrations and the tested contributing components during the period from 15th to 30th August 2011, excluding the rainy days (18th -22nd August). The orange shadow (14:00-18:00) indicates daily O₃ peak time.

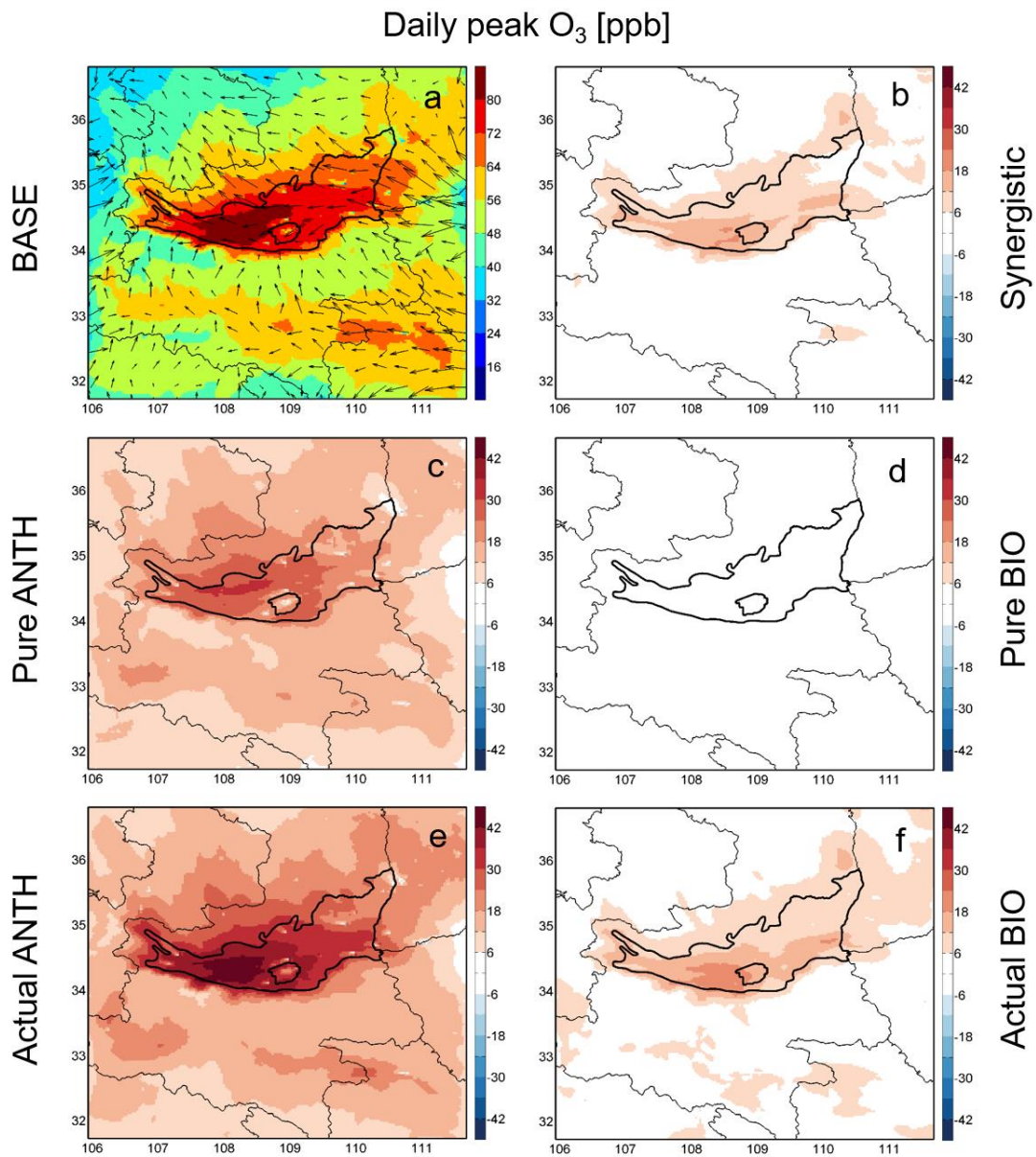


Figure 8. Spatial distributions of monthly mean concentrations of daily peak O₃ in August 2011. (a) is the result from the BASE simulation, overlaid with simulated wind vectors. (b)-(f) are simulated daily peak O₃ concentrations contributed from synergistic anthropogenic and biogenic, pure anthropogenic, pure biogenic, actual anthropogenic and actual biogenic sources, respectively.

5

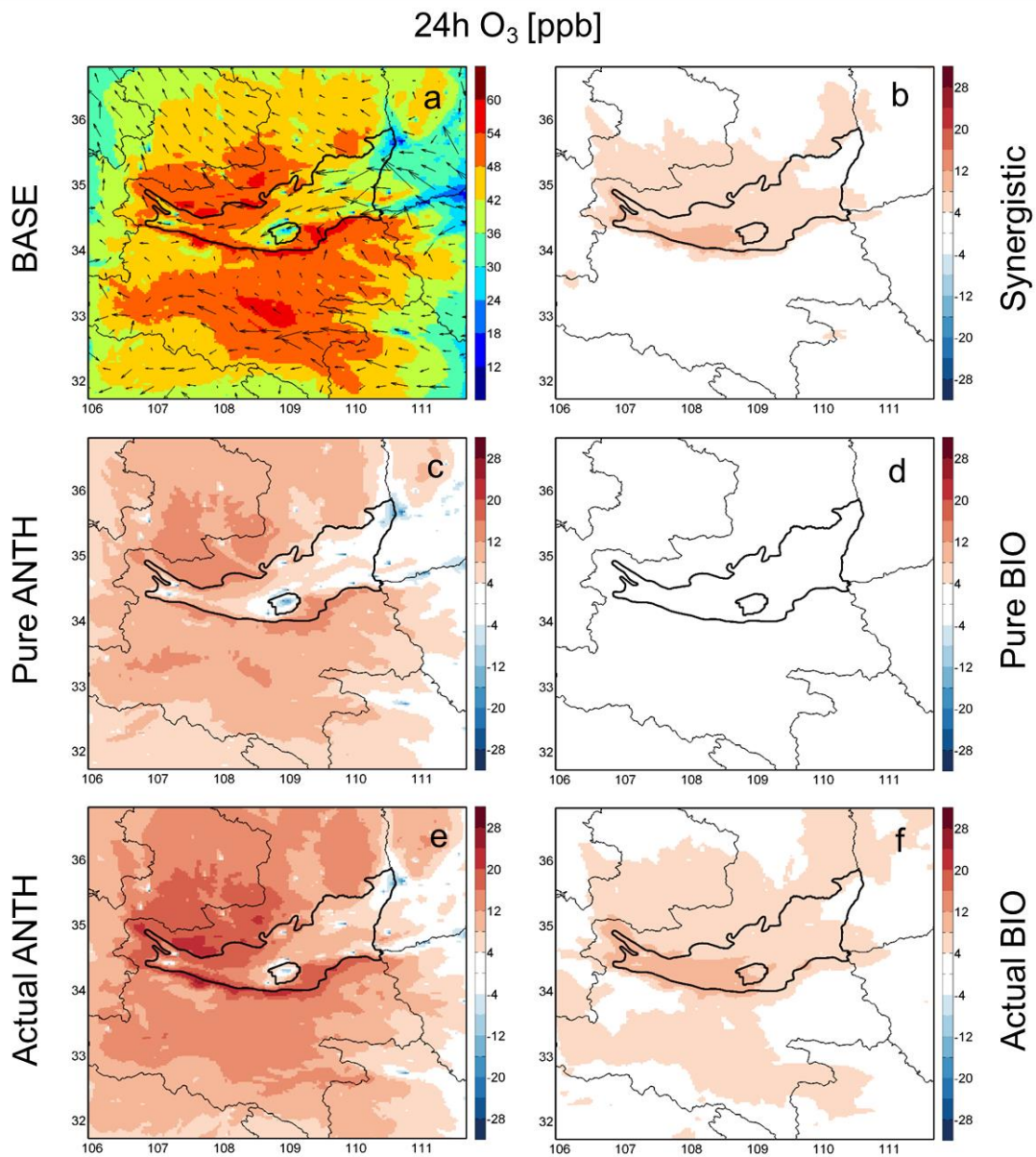


Figure 9. Spatial distributions of monthly mean concentrations of 24h averaged O₃ in August 2011. (a) is the result from the BASE simulation, overlaid with simulated wind vectors. (b)-(f) are simulated 24h averaged O₃ concentrations contributed from synergistic anthropogenic and biogenic, pure anthropogenic, pure biogenic, actual anthropogenic and actual biogenic sources, respectively.

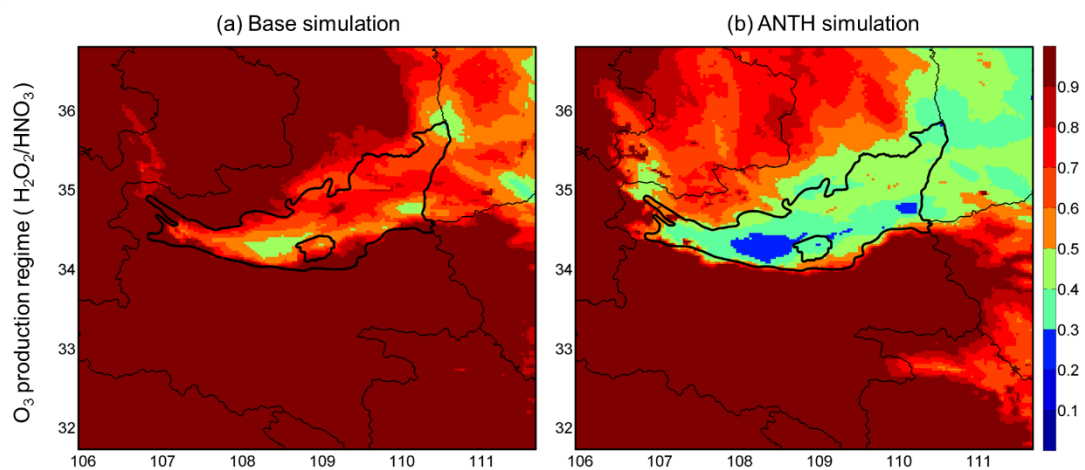


Figure 10. The monthly mean ratio of $\text{H}_2\text{O}_2/\text{HNO}_3$ during the daily O_3 peak time (14:00-18:00 local time) in August 2011 in the (a) Base simulation and (b) the simulation without biogenic sources.

5

Table 1. Ambient biogenic VOCs observations in the Qinling Mountains during 6th – 7th August 2011

Site ^a	Date	Start Time ^b	Location	Isoprene (ppb)		Monoterpenes (ppb)		Dominant monoterpenes ^c
				Observation	Simulation	Observation	Simulation	
NBL	2011/8/6	10:20	33.78 E, 108.88 N	3.8	4.5	0.42	0.29	α -pinene
ZA	2011/8/6	12:44	33.40 E, 109.05 N	0.1	0.9	0.16	0.22	α -pinene, limonene, menthone
XY	2011/8/6	16:14	32.87 E, 109.40 N	1.0	0.3	0.24	0.13	α -pinene
AK	2011/8/7	09:45	32.71 E, 109.01 N	0.8	0.4	0.10	0.08	α -pinene
TJB	2011/8/7	13:00	32.99 E, 107.78 N	0.5	1.1	0.27	0.26	α -pinene
YS	2011/8/7	14:50	33.27 E, 107.73 N	1.6	0.9	0.04	0.32	α -pinene
Average				1.3	1.4	0.21	0.22	

^a Site names: NBL (Niubeiliang), ZA (Zhenan), XY (Xunyang), AK (Ankang), TJB (Tangjiaba), YS (Youshui)

^b The sampling duration is 30 minutes.

^c Other monoterpenes detected (0.1% to 9%) include tricyclene, α -thujene, camphene, sabinene, myrcene, α -phellandrene, Δ -carene, o-cymene, β -ocimene, cineole, isopulegol, isomenthone.

Table 2. Summary of different simulation settings and definitions of the various contributions from anthropogenic and/or biogenic sources.

Simulation	Simulation results	Anthropogenic emission	Biogenic emission
BASE	$f_{\text{anth-bio}}$	✓	✓
ANTH	f_{anth}	✓	✗
BIO	f_{bio}	✗	✓
NEITHER	f_0	✗	✗
Contribution			
	$f_{\text{anth-bio}} - f_{\text{bio}}$	Actual contribution of anthropogenic emissions	
	$f_{\text{anth-bio}} - f_{\text{anth}}$	Actual contribution of biogenic emissions	
	$f'_0 = f_0$	The contribution of background transport	
	$f'_{\text{anth}} = f_{\text{anth}} - f_0$	Pure contribution of anthropogenic emissions	
	$f'_{\text{bio}} = f_{\text{bio}} - f_0$	Pure contribution of biogenic emissions	
	$f'_{\text{anth-bio}} = f_{\text{anth-bio}} - (f_{\text{anth}} + f_{\text{bio}}) + f_0$	Synergistic contribution of anthropogenic and biogenic emissions	

Table 3. Statistics of meteorological and air quality variables over the GZ basin in August 2011^a

	Mean		r ^d	NMB ^d	RMSE ^d
	Observation	Simulation			
Meteorology^b					
Wind speed (m s ⁻¹)	2.6	2.5	-	-6%	1.8
Temperature (°C)	25.1	24.2	0.86	4%	2.5
Relative humidity	73.6%	74.2%	0.72	1%	12%
Air quality^c					
NO _x (ppb)	47.0	46.6	0.36	-1%	18.1
O ₃ (ppb)	31.5	38.7	0.72	21%	8.1
PM _{2.5} (µg m ⁻³)	107	94.6	-	-12%	49.3

^a Averaged for the period from 15th to 30th August 2011, excluding the rainy days.

^b Meteorological data were obtained from the hourly surface measurements at Jinghe station (108.58 °E, 34.26 °N)

^c Air quality data were measured at the roof (107 m above ground) of the main building (108.98 °E, 34.25°N) on the campus of Xi'an Jiaotong University

^d r: correlation coefficient; NMB: normalized mean bias; RMSE: root mean square errors.

Table 4. The various contribution components of the simulated O₃ (and the precursors) and PM_{2.5} in August 2011

	NO _x [ppb]	VOCs [ppb]	O ₃ [ppb]		PM _{2.5} [μg m ⁻³]
			daily peak ^a	24h	
<i>The GZ basin</i>					
Base	11.1	24.5	74.1	44.4	65.1
Pure ANTH	11.0	8.0	22.6	5.0	52.0
Pure BIO	0.1	9.9	2.0	1.1	3.3
Actual ANTH	10.6	7.7	33.0	10.8	53.5
Actual BIO	-0.3	9.6	12.5	7.0	4.9
Syn ANTH-BIO	-0.4	-0.3	10.5	5.8	1.5
<i>Urban Xi'an</i>					
Base	30.1	44.8	74.7	38.7	102
Pure ANTH	30.3	26.4	19.1	-2.2	88.7
Pure BIO	0.15	12.4	2.6	1.4	3.4
Actual ANTH	29.6	26.2	33.4	4.6	91.1
Actual BIO	-0.6	12.2	16.8	8.2	5.8
Syn ANTH-BIO	-0.7	-0.2	14.3	6.8	2.4

^a Daily O₃ peak time is from 14:00 to 18:00 local time